Diplomarbeit

Optical coherence tomography evaluation of Single String bifurcation stenting technique

eingereicht von

Bellmann Frederik

zur Erlangung des akademischen Grades

Doktor der gesamten Heilkunde

(Dr. med. univ.)

an der

Medizinischen Universität Graz

ausgeführt an

der Klinischen Abteilung für Kardiologie

unter der Anleitung von

Prof. Dr. med. univ. Robert Zweiker

Dr. med. Gábor G. Tóth-Gayor

Graz, 25.07.2016

Eidesstattliche Erklärung

Ich erkläre ehrenwörtlich, dass ich die vorliegende Arbeit selbstständig und ohne fremde Hilfe verfasst habe, andere als die angegebenen Quellen nicht verwendet habe und die den benutzten Quellen wörtlich oder inhaltlich entnommenen Stellen als solche kenntlich gemacht habe.

Graz, am 25.07.2016 ..... Bellmann Frederik eh

Danksagung

Ich möchte mich recht herzlich bei Herrn Prof. Dr. Robert Zweiker bedanken, durch welchen ich die Möglichkeit hatte, meine Diplomarbeit an meiner Wunschabteilung zu verfassen. Außerdem gilt mein Dank Herrn Dr. Gabor Toth-Gayor, der mir immer mit Rat und Tat zur Seite stand und mir den Zugang zu meinem Thema erleichtert hat.

Mein besonderer Dank geht an meine Eltern, Gisela und Werner, sowie Hildegard, ohne welche ich heute nicht da wäre wo ich bin und deren moralischer und finanzieller Beistand mein Studium überhaupt erst ermöglicht und mir eine unbeschwerte wie auch unvergessliche Zeit in Graz beschert hat.

HERZLICHSTEN DANK!

Arbeiter der Stirn

Ein Mensch sitzt kummervoll und stier
Vor einem weißen Blatt Papier
Jedoch vergeblich ist das Sitzen –
Auch wiederholtes Bleistiftspitzen
Schärft statt des Geistes nur den Stift.
Selbst der Zigarre bittres Gift,
Kaffee gar, kannenvoll geschlürft,
Den Geist nicht aus den Tiefen schürft,
Darinnen er, gemein verbockt,
Höchst unzugänglich einsam hockt.
Dem Menschen kann es nicht gelingen,
Ihn auf das leere Blatt zu bringen.
Der Mensch erkennt, dass es nichts nützt,
Wenn er den Geist an sich besitzt,
Weil Geist uns ja erst Freude macht,
Sobald er zu Papier gebracht.

Eugen Roth

Zusammenfassung

Hintergrund

Seit dem Beginn der interventionellen Ära in der klinischen Kardiologie, angefangen bei der ersten erfolgreichen perkutanen Koronarangioplastie im Jahr 1977, welche von Andreas Grüntzig durchgeführt wurde, und der ersten Stentimplantation in eine menschliche Koronararterie durch Jacques Puel und Ulrich Gigwart im Jahr 1986, hat eine fortlaufende Weiterentwicklung bezüglich eingesetzter Stentmaterialien sowie angewandter Implantationstechniken stattgefunden. Auch wenn das Koronarstenting seitdem extreme Fortschritte gemacht hat und, im Falle von unkomplizierten Einfachläsionen, zu einem routinemäßigen Eingriff geworden ist, so bleibt die simultane Anwendung von zwei oder mehr Stents, was sich bei Bifurkationsläsionen häufig als der zielführendste Ansatz herausgestellt hat, immer noch eine Herausforderung. Über die Jahre wurden viele Verfahren entwickelt, welche immer das Ziel hatten, Überlappung oder Deformierung der Stentstreben zu minimieren und die möglichst nah an die Gefäßwand anliegende Positionierung des Stents zu optimieren. Um diesen Ansprüchen bestmöglich gerecht zu werden, wurde ein neuer Verfahrensweg vorgestellt, welcher Single String Stenting Technik genannt wird. Diese Arbeit wird sich im Folgenden damit beschäftigen, ob eine Überlegenheit des neuen Verfahrens gegenüber den bereits etablierten Zwei-Stent Techniken gegeben ist.

Material & Methoden

In dieser Studie wurden 13 Patienten mit komplexen Bifurkationsläsionen inkludiert, bei welchen sowohl der Hauptstamm (MB) als auch der wichtige Seitenast (SB) betroffen war. Die Evaluierung der Stentpositionierung und Entfaltung wurde mittels intrakoronarem optical frequency domain imaging (OFDI) durchgeführt. Für die Bildauswertung wurde die Terumo Lunawave Console verwendet. Die Analyse der Stententfaltung und Positionierung (engl. = apposition) wurde in allen postinterventionellen Durchläufen des Hauptstammes sowie bei 5 Fällen des Seitenastes durchgeführt. Die Werte der Distanzmessungen zwischen Stentstrebe und Gefäßwand wurden in einem Excel Arbeitsblatt zusammengefasst und hinsichtlich der Zielgröße

“Appositionierungsgrad” statistisch ausgewertet. Hierbei wurde eine perfekte Apposition als ein Gefäß-Streben-Abstand von 0µm und Malapposition als ein Gefäß-Streben-Abstand von größer 200µm definiert.

Ergebnisse

Alle 13 in vivo Eingriffe wurden erfolgreich gemäß dem Protokoll durchgeführt, wobei nur bei 5 Patienten ein kompletter Datensatz, inklusive OFDI des Seitenastes, verfügbar war. Im Falle der anderen 8 Patienten konnte nur der Hauptast ausgewertet werden. Insgesamt wurden 465 OCT Frames analysiert und 6370 Stentstreben als solche identifiziert und evaluiert. Bezogen auf alle sechs Bifurkationssegmente, waren in Summe 3405 Streben (67%) perfekt appositioniert. Dagegen wurden 406 Streben (8%) als malappositioniert identifiziert. Im besonders wichtigen Ostiumbereich des Hauptstammes, zeigten 1665 Streben (59%) perfekte Apposition und 329 (12%) eine Malapposition.

Conclusio

In dieser Studie konnte die klinische Durchführbarkeit der Single String Stenting Technik klar gezeigt werden. Das Verfahren war bei allen Studienteilnehmern durchführbar und es gibt grundsätzlich keine Einschränkungen bezüglich der Anwendbarkeit dieser neuen Stentingtechnik mit konventionellen Stentmaterialien kommerzieller Hersteller. Die Malappositionsraten, die diese Studie liefern konnte, sind grundsätzlich sehr vielversprechend, auch wenn die Vergleichbarkeit der Ergebnisse mit anderen Zwei-Stent Techniken, auf Grund abweichender Messmethoden und Zielgrößendefinition, nicht hundertprozentig gegeben ist. Zum jetzigen Zeitpunkt kann keine Aussage über weitere wichtige Einflussgrößen wie z.B. Gefäßwanddeckung oder Stentüberlappung, getroffen werden. Um eine endgültige Entscheidung darüber treffen zu können, inwieweit dieses neue Verfahren den konventionellen Stentingmethoden überlegen ist, wird eine direkte Vergleichsstudie mit ähnlichen Studienkollektiv und übereinstimmenden Zielgrößen nötig sein.

Abstract

Background

Since the beginning of the interventional era in cardiology starting with the first successful percutaneous coronary angioplasty in 1977 performed by Andreas Grüntzig and the first stent deployment into a human coronary artery in 1986 by Jacques Puel and Ulrich Sigwart, there has been a continuous development in terms of types of materials used as well as the applied techniques for the stent deployment. As advanced and controllable coronary stenting has become for uncomplicated single lesion treatment, the simultaneous application of two or more stents, which is often seen as the most expedient approach in case of bifurcation lesions, remains a challenge. Over the years many techniques have evolved, always for the purpose of minimizing stent overlap or distortion as well as optimizing the stent apposition and its wall coverage. In order to meet these requirements as much as possible, a new approach called the Single String stenting technique was introduced. The purpose of this diploma thesis is to determine, weather the superiority of this method with regard to the above mentioned variables towards the other established two-stent techniques (Culotte, Crush, Mini-crush) is warranted or not.

Material & Methods

13 Patients with complex bifurcation lesions (involving both the main branch and an important side branch) were included in this trial. For the evaluation of the stent deployment, intracoronary optical frequency domain imaging (OFDI) was used. The image analysis was performed using the Terumo Lunawave console. For the analysis of the stent strut apposition, the post-interventional runs of each bifurcation lesion, including main- and side branch, were selected. All distance measurements of the stent struts were transferred into a Microsoft Excel sheet and analyzed in regard to the target values which were defined as perfect apposition with a strut-vessel wall distance of 0µm as well as marked malapposition with a distance of more than 200µm.

Results

All 13 in vivo procedures were successfully performed according to the protocol, whereas only in five cases, the complete data of two post-interventional OFDI pull-back runs, namely the MB and the SB run, were available. Regarding the other eight cases, only the MB but not the SB could be analyzed. In all 13 cases, a total number of 465 OCT frames was analyzed and 6370 stent struts were identified for evaluation. All six bifurcation segments considered, an overall number of 3405 stent struts (67 %) showed perfect apposition (=0 µm), whereas marked malapposition (>200µm) was seen in 406 struts (8%). In the important ostial area of the main-branch, 1665 Stuts (59%) were perfectly apposed and 329 (12%) showed marked malapposition.

Conclusions

In this study the feasibility of the single string stenting approach was clearly demonstrated. The procedure was applicable for all participating patients and for this technique, there are basically no limitations regarding the type of stent or the manufacturer. In general, the rates of malapposition this trail yielded are favorable, even if the comparability with the result of other double-stent techniques are not fully possible, due to deviating measurement techniques and the different definition of the target values.

At this point, there is no further prediction regarding other important factors like wall coverage and stent overlap possible. In order to be able to draw a final conclusion about the superiority of single string stenting technique towards other double-stent techniques, a comparative clinical trial with an appropriate study size and matching study parameter will be necessary.

Contents

1 Introduction

1.1 Coronary artery disease

1.1.1 General overview

Coronary artery disease (CAD), often referred to as coronary heart disease, atherosclerotic cardiovascular disease, or ischemic heart disease encompasses a large group of clinical manifestations due to the narrowing of coronary arteries caused by pathological alterations of the vessel wall. As a consequence, an imbalance between the blood consumption of the heart muscle and the supply provided by the coronary circulation is developed which subsequently leads to a shortage of oxygen in the myocardial cells. This imbalance can present in a variety of clinical pictures, depending on what triggers this lack of blood supply. The most common syndromes, such as instable angina, myocardial infarction and sudden cardiac death, are subsumed under the term of “acute coronary syndrome (ACS)”. Even though there exist different pathologic mechanisms underlying the occurrence of these syndromes, coronary atherosclerosis is by far the principle cause of CAD. Because of this fact, it is important to understand the etiology and pathogenesis of atherosclerosis and the impact of these morphological alteration on the development of clinical symptoms. Only by coming to the roots of this disease, it is later possible to discuss the adequate treatment options. [1, 2]

1.1.2 Coronary atherosclerosis

1.1.2.1 Etiology

Atherosclerosis is a chronic inflammatory vascular disease [3] with a very complex and multifactorial pathogenesis, which makes it still not a completely understood process. According to the current knowledge, the response-to-injury hypothesis is the most widely accepted concept. In this theory postulated by Russell Ross, an injury of the endothelium initiates a number of pathological processes, which will ultimately lead to the development of atheromatous plaques and calcifications [1]. There are many factors which cause the endothelial damage and predispose for the

atherogenesis. The traditional risk factors are hyperlipidemia, diabetes mellitus, hypertension, advanced age, male sex and cigarette smoking although none of those are sufficient to cause atherosclerosis by itself [4]. The key role in the pathogenesis of this disease plays the dysfunctional lipid metabolism and the resulting abnormal composition of the serum lipids, especially elevated levels of low density lipoprotein (LDL). Only if dyslipidemia is present, can the other factors contribute to raise the chance of developing atherosclerosis. This proposition rests upon 4 known facts:

1) In an experiment conducted with nonhuman herbivores in the early 20th century, it was shown that by feeding them high-cholesterol fat, 100% were developing atherosclerosis. But this was not the case when their blood pressure and blood glucose levels were raised artificially or when they had been exposed to cigarette smoke throughout life.

2) Cholesterol, which constitutes the largest part of the LDL particle can be found in the plaques.

3) Probably the most known fact is that populations with relatively high serum cholesterol levels due to the hypercaloric diet with a lot of saturated fatty acids and cholesterol show a higher frequency of atherosclerotic events as well as an increased mortality when they occur.

4) The therapeutic effect of LDL lowering drugs has been proven by the reduction of these events and the positive effect on the plaque size.

These examples show the importance of low density lipoprotein in the genesis of plaques [5]. Another acknowledged risk factor for atherosclerosis are genetic alterations. If there are genes affected that are coding for any proteins involved in the lipid metabolism, it is possible that the individual develops a non-environmentally acquired hyperlipidemia. But also genes that are responsible for the coagulation factors and endothelial NO-synthase can be mutated and facilitate alterations of the vessel wall [4].

1.1.2.2 Pathophysiology

As mentioned before, injuries of the endothelium provide the starting point for further remodeling processes of the Intima. Based on that, complex interactions between

the vessel wall and soluble as well as formed blood components take place. The destruction of the endothelial integrity enables the influx of plasma LDL into the intima. This accumulation of cholesterol is still reversible, because the body uses another lipoprotein, called high density lipoprotein (HDL) to remove unnecessary LDL from the periphery and transport it back to the liver. However, this reverse transport and the uptake of LDL is only functioning because of special cell surface receptors on both lipoproteins. The problem is that the accumulated LDL is being modified by several different methods in a way that it also uses another receptor pathway. The two most significant modifiers are reactive oxygen species (ROS) and products of the nonoxidative glycation in diabetes mellitus. ROS are mainly generated extracellularly by macrophages and endothelial cells by stimulation of TNF-alpha and other cytokines. The intracellular production takes place in the vascular smooth muscle cells (VSMC) through the membrane-bound NAD(P)H oxidases, xanthine oxidase and uncoupled NO synthase. Nonenzymatic glycation is the second very complex mechanism, which results in the formation of advanced glycation end products (AGEP). These molecules again accelerate the oxidation of HDL, LDL and VLDL. After the oxidation of LDL is performed, the then called oxLDL induces the expression of cell surface adhesion molecules in endothelial cells which mediates the adhesion of monocytes and T-lymphocytes. After their migration into the intima guided by cytokines, the monocytes differentiate into macrophages. Through the scavenger receptor pathway, the oxLDL is internalized by the macrophages turning them into lipid-rich foam cells. At this stage the modifications of the vessel wall appear macroscopically as “fatty streaks”. Cytokines and other mediators (platelet derived growth factor-like molecules) produced by the macrophages and T-lymphocytes lead to the recruitment and proliferation of vascular smooth muscle cells which migrate from the media to the intima. As a consequence of the apoptotic death of foam cells, a central core of extracellular lipid and necrotic debris is formed. As the plaque grows, immigrated smooth muscle cells create a connective tissue matrix which forms the fibrous capsule of the plaque. Additionally the plaque can contain calcifications or cholesterol crystals. Regardless of having a luminal stenosis or not, the lesion is than considered to be an “advanced lesion”. [3, 4, 6–8]

In the initial period the plaque is growing abluminal, which makes it hard to detect by angiographic methods. As the disease advances, the plaque growth is facilitated by the enrichment of necrotic material within the core and the intraplaque hemorrhage. This may result from either the influx of blood from the vessel lumen through fissures due to the erosion of the fibrous cap or from leakage of the intraplaque vasa vasorum, which originate in the course of the structural organization of the plaque [9, 10]. The further the atherosclerotic disease progresses, the bigger the chance of intraluminal expansion of the lesion, which may be in an eccentric or concentric pattern. In order to keep an adequate blood flow despite the stenosis, the vessel wall is being remodeled, mainly by vasodilatation [6, 8].

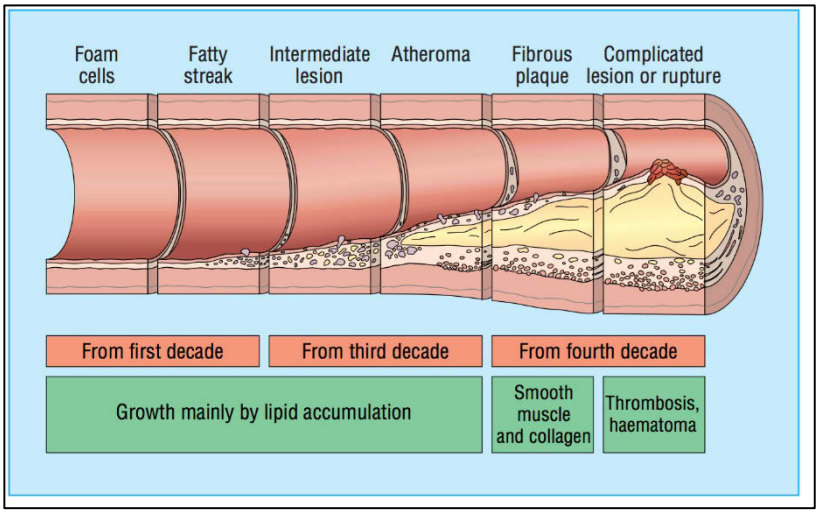

Fig. 1: Progression of an atherosclerotic lesion

1.1.2.3 Plaque rupture

This fibrous cap has the important task of keeping the highly thrombogenic content of the plaque separated from the blood stream, especially the platelets [11]. Depending on the thickness and the integrity of the cap, the plaque can be relatively stable or unstable, which is then called a vulnerable plaque characterized by its higher risk to rupture. A thickness of the cap measuring less than 65 micrometers, a relatively large necrotic core plus the distinct infiltration of macrophages and lymphocytes are the criteria for a vulnerable plaque, today designated as a thin-cap

fibroatheroma (TCFA). TCFAs are the precursor lesions of ruptured plaques differentiating them from their smaller necrotic core and fewer macrophages as well as fewer calcifications [9]. Macrophages play a central role in inflammatory process of weakening the fibrous capsule. They produce matrix metalloproteinases (MMP), a group of enzymes which are able to actively destroy extracellular matrix. Moreover, T-lymphocytes stimulate the secretion of these endopepdidases by the macrophages and also inhibit the synthesis of collagen I and III by the SMC via interferon so that the extracellular matrix is further decreasing. Another aspect is the mechanical stress due to physiological blood pressure alterations, pathologically elevated blood pressure or vascular spasm, which may lead to plaque rupture especially if the cap has been previously damaged. The fact that the lesion ruptures more frequently at the proximal site of the stenosis where the hemodynamic shear stress is higher than poststenotically, validates this observation. The final result of these destabilizing processes is the disruption of the vulnerable plaque with exposure of lipids, necrotic debris, and collagen to the blood stream. Collagen triggers the activation of the platelets and their aggregation at the site of the lesion. [11, 12]

The formed thrombus can be mural (nonocclusive) or occlusive, depending on the extent of the disruption. At the beginning it is called a white thrombus, because it is mainly composed of platelets. The longer the ischemic time duration gets, the more erythrocytes and fibrin will be found in the then called red thrombus. [8, 9]

1.1.3 Stable angina

Both the atherosclerotic narrowing and the coronary thrombosis can reduce the lumen of the artery and therefore the blood flow. Depending on whether the stenosis develops acutely as with an occluding thrombus or over a longer period of time like a fibrous plaque, the patient presents different symptoms. Angina pectoris, which is derived from the Latin words “angere” (to strangle) and “pectus” (chest), is a clinical term describing chest discomfort due to coronary hypoperfusion and consequential oxygen deficiency. Symptoms of stable angina are precordial tightness or pain which are provoked by physical exertion and emotion but typically relieved by rest or nitroglycerin. The pain can spread as far as the left arm, epigastrium and jaw or neck area [13]. Because of the causality and reproducibility of these symptoms this

syndrome is called stable angina whereas in the majority of the cases, the pathological correlate is coronary atherosclerosis. Because the arteries are dynamic in nature, they are able to dilate and therefore compensate the luminal narrowing until a certain level and maintain a sufficient blood flow. The threshold of cross-sectional luminal narrowing that is needed before the blood flow is affected is about 75%. A stenosis that causes near maximal vasodilatation during resting conditions is called a critical stenosis. [8, 14]

1.1.4 Acute coronary syndromes

Angina that occurs for the first time or suddenly in rest is indicative of unstable angina (UA) which is usually caused by plaque rupture and subsequent intracoronary thrombosis [10]. The thrombus leads to an acute subtotal stenosis of the artery, which is already constrained by the plaque and maximally dilated. This hemodynamically relevant stenosis causes an immediate shortage of oxygen in the myocardial area that this artery feeds and provokes similar symptoms like stable angina. If these episodes last longer than 30 minutes and are associated with more severe chest pain, there is a high risk that it may be a myocardial infarction (MI) which would mean that the artery is completely occluded. The primary difference between UA and MI is that the latter causes an ischemia severe enough to result in a necrosis of the myocardium which releases specific cardiac enzymes like Troponin I, T and CK-MB into the blood stream. Because of the fact that both the UA and the MI (NSTEMI) can impose with ST-flattening or depression in the ECG, the exact differentiation requires the measurement of these cardiac enzymes. The problem is that a detectable elevation of troponin takes up to 6 hours making it difficult to distinguish between UA and NSTEMI in the initial period. An acute MI occurs if the ischemic time duration exceeds about 20 minutes. Because the perfusion of the heart muscle proceeds from the epicardium to the subendocardium, this inner wall is the location where the infarct begins. For the first two hours the area of the infarct is limited to the subendocardium (NSTEMI) but it will extend towards the epicardium if the ischemia persists. The result is a transmural necrosis that creates a ST-segment elevation in the relative lead of the ECG. At this stage the infarct is called a ST-segment elevation myocardial infarction (STEMI). [15][16]

The third syndrome of acute coronary events where CAD constitutes the leading cause is the sudden cardiac death (SCD). It is defined “as an unexpected natural death from cardiac cause that occurs spontaneously or within 1 h from the onset of abrupt change in clinical status in a person without a prior condition that would have appeared to be fatal”. The ischemia triggered by the atherosclerotic plaque or the coronary thrombosis leads to a lack of oxygen in the cells of the myocardium and the cardiac conduction system which produces a calcium overload, a decrease in pH and an inhibition of the sodium-potassium pump. This results in delayed afterdepolarization and ultimately in ventricular fibrillations, a lethal condition if it is not treated. [17]

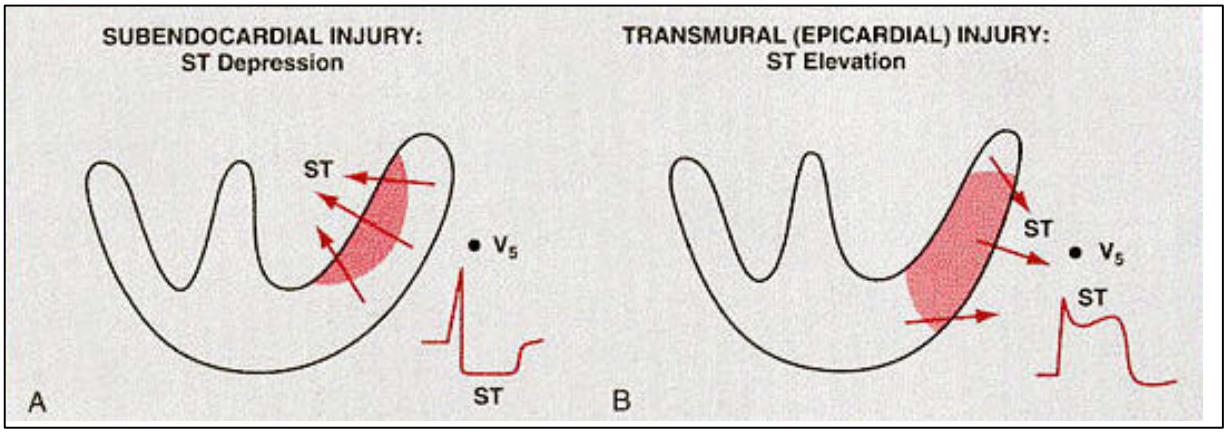

Fig. 2: ST-depression (a), ST-elevation (b)

1.2 Percutaneous coronary intervention

1.2.1 Coronary angiography

Prior to every percutaneous coronary intervention (PCI), which is a term for a minimally invasive non-surgical procedure that is performed on patients suffering from CAD to treat the narrowing of the coronary arteries, a coronary angiography is obligatory for the thorough assessment of the severity of CAD. The primary goal of this diagnostic procedure is to identify and localize the stenotic lesions and their extent within the coronary arteries. The result of this imaging technique will determine whether or not PCI is indicated and technically feasible. For this minimally invasive procedure, the patient is placed on the operating table in the catheter laboratory. Proper sedation is necessary to keep the patient calm and compliant enough to

follow instructions for inspiration, breath-holding, or expiration, which can facilitate certain maneuvers during the angiography or a potential PCI. The former most commonly used approach is the percutaneous transfemoral technique, whereby the radial access is increasingly applied as a routine approach. In the former case, the left common femoral artery is punctured with a thin-walled needle after the skin and subcutaneous tissue at the puncture site have been injected with a local anesthetic. The next step is to insert a 0.89 mm J-tipped guidewire through the needle into the arterial lumen and to push it forward to the ascending aorta with the tip placed at the level of the coronary ostia. Afterwards the needle is removed and by using the wire as a guide rail, a short tube with a one-way valve, called introducer sheath, is advanced into the artery. The size of the sheath should be chosen corresponding to the diameter of the diagnostic catheter or a possible interventional device. For the angiogram, an Amplatz or Judkins catheter are used. These catheters are constructed of polyurethanes and polyethylenes with a special wire braiding, which gives them the important property of shape retention and torque transmission. Their caliber is measured in French (F) size, which complies with the circumference in millimeters (1F = 1/3 mm) and they are available in sizes from 4-6 French. The catheter is inserted through the introducer sheath and should be advanced into the ascending aorta by the help of the guidewire to prevent any arterial dissection. In order to clear the catheter from air or debris, aspiration is necessary before the contrast agent can be applied. After the cannulation of the left or, as the case may be, right coronary ostium, the contrast medium is injected into the arteries either by a motorized injector or manually with a syringe. Iodine is the essential compound of the most commonly used contrast agents because it absorbs x-ray photons. Due to its high osmolality and content of iodine it can lead to unwanted effects like allergic reactions, toxic effects or ventricular arrhythmias. Because of the fact that it has a high iodine concentration and is primarily excreted by renal glomerular filtration, it can cause thyroid and kidney dysfunction. This is why nonionic and nearly iso-osmotic agents have been developed showing a significant reduction of the above-named side effects.

For the visualization of the coronary arteries a radiographic imaging system is used. Therefor the X-ray tube and the image detector are mounted on a moveable C-arm, so that the image of the blood vessels can be acquired in various projections, which

is important to demonstrate the narrowing lesions in true profile. In order to reduce the radiation exposure and to obtain a sharp image despite the heart contractions, a fast pulsed X-ray beam is required. With an image acquisition frequency of 15 frames/s, a relatively smooth live view can be produced. [18–20]

1.2.2 Interventional treatment modalities

The result of the coronary angiography decides whether the indication for a PCI is given or not. Depending on the quantity, the location and the morphology of the stenotic lesion, different interventional treatment modalities are used to provide the best possible outcome. The arterial access and the first steps until the guidewire is placed in the ascending aorta are similar to the angiographic procedure.

1.2.2.1 Balloon angioplasty

Balloon angioplasty, formerly referred to as percutaneous transluminal coronary intervention (PCI) is an interventional method that is used to distend and therefore enlarge the segment of artherosclerotically altered coronary arteries with a constrained lumen. For this purpose, the guiding catheter is placed in the coronary ostium in question and a 0.014-in diameter radiopaque guidewire is inserted and advanced to the narrowing lesion. Then, the wire is eased through the stenosis with the wire tip positioned distally. Following this, the balloon catheter is slid over the guidewire and placed right between the thickened artery walls. Using a pressure of 10-16 atm (1 atm equals 760 mmHg), the balloon is inflated with a radiopaque fluid for 20-60s. This causes a distension of the artery with an immediate increase of the lumen diameter. By inflating the balloon, a semi-controlled artery dissection is induced, which lets the plaque rupture and is often accompanied by fissures in the internal elastic lamina involving a hematoma of the media. Compression of the plaque, initiation of the healing process and expansion of the outer artery diameter are the main factors increasing vessel lumen. The arterial diameter can improve extremely various, but averages about 250%.

Acute complications like vascular spasm, downstream embolization of plaque material and chronic complications especially restenosis may also occur after several weeks. [18]

1.2.2.2 Coronary artery stenting

In order to prevent acute complications and to reduce the risk of restenosis, stent implantation has become an efficient adjunct to balloon angioplasty. The initially used stents were stainless steel tubes with a meshed structure put onto a balloon at the tip of a catheter. Today's cobalt chromium stents allow a slimmer design and provide more longitudinal flexibility as well as radial strength while having a reduced wall thickness. Compared to the first generation of stents, they are not as bulky and can even be placed in severely narrowed artery lumens. Still, metal alloy stents pose a risk of thrombosis due to the thrombogenicity of any artificial implant and the lumen-loss caused by a 400-micrometer thick layer of fibrotic tissue covering the metal framework, which makes it a total reduction of the cross-section diameter by 800 micrometers. This fact led to an improvement in stent development made by adding a drug-embedded polymer stent strut coating, which releases a constant amount of antiproliferative drugs. These drug eluting stents (DES) can contain two families of drugs: immunosuppressants like Sirolimus, Everolimus, Zotarolimus or the cancer chemotherapy drug Paclitaxel. With DES it is possible to minimize the diameter lumen-loss to approximately 150-300 micrometer. The incidence of clinically relevant restenosis was reduced to 4-8% which is a major advancement compared to the bare-metal stents (BMS) with about 20%. The proceeding of placing the stent follows almost the same steps as described with balloon angiography. A special catheter is used, where the stent is crimped onto a balloon. After the unevolved stent is positioned in the narrowed part of the artery, the stent is deployed by inflating the balloon which lets the metal framework expand, starting at the distal ending. The stent should be apposed correctly to the vessel wall on its entire circumference in order to seal the disrupted intima, to obtain the maximally possible lumen diameter and to facilitate the development of the neo-intima covering the stent struts.[18] [21]

1.2.2.3 Thrombectomy

Thrombectomy is a method for transcatheter thrombus removal, which is often used in case of acute myocardial infarction to reduce the risk of downstream embolization. PCI performed in patients with acute coronary syndrome caused by coronary thrombosis on the basis of a ruptured atherosclerotic plaque can cause the embolization of a clot. The removal of the thrombus before further interventional treatment reduces the complications and the mortality risk. There are two methods of thrombectomy, one using a simple aspiration catheter, or the second way, by using a catheter which mechanically aspirates and disrupts the thrombus. Both catheters are inserted into the coronary artery where the thrombotic lesion is located with the help of a standard coronary guidewire. In the first case, a syringe is attached to the end of a thin-wall catheter with small holes at the distal lumen. While advancing the catheter through the lesion, the doctor manually aspirates the clot with the syringe. The second method uses a special catheter that has a lumen for a high-pressure saline jet. This jet creates a suction at the tip of the catheter which is able to macerate the clot after it has been aspirated. Compared to the simple thrombectomy, there is no improved outcome. [18]

1.2.2.4 Atherectomy

Atherectomy is a transcatheter technique to remove intraluminal tissue by abrasion or cutting which has very limited indications due to its relatively high complication rate. Still, it is a useful device when it comes to pretreatment of severely calcificated lesions or stenosis located at a coronary bifurcation, which are both factors that can make PTCA and stent placement hard or even unfeasible. There are two devices available, whereby each of them uses another plaque removing technique. The first method is called directional atherectomy (DCA). At the tip of the catheter is a cylindrical metal housing with a small window measuring 9-16mm which will be positioned facing the lesion. On the opposite side of the cylinder, an inflatable, non-compliant balloon is attached. Inside of the metal cone is a rotating blade which is connected by a drive cable to an external motor running at approximately 2000 rpm. After the cutting window has been placed in front of the plaque, the balloon is inflated pushing the protruding plaque into the cutting chamber of the metal cylinder. The

rotating blade is switched on and the ablated tissue is deposited within the nose cone. In order to get a complete, circumferential removal, the balloon has to be deflated, the window slightly rotated and then reinflated. This procedure is repeated until the entire lesion is abraded. The second method is called rotational atherectomy which works on the concept of drilling. The catheter has an elliptical burr coated with 20–50 μm diamond microparticles at its tip. The burr is rotating at approximately 160 000 – 200 000 rpm driven by an external air turbine. Due to the high rotating speed and the extremely fine diamond coating, the abraded particles are smaller than 5 μm, which is too small to cause any downstream embolization. However, complications like micro-cavitation bubbles, dissection and perforation are possible. [18, 21]

1.3 Reperfusion strategy algorithm

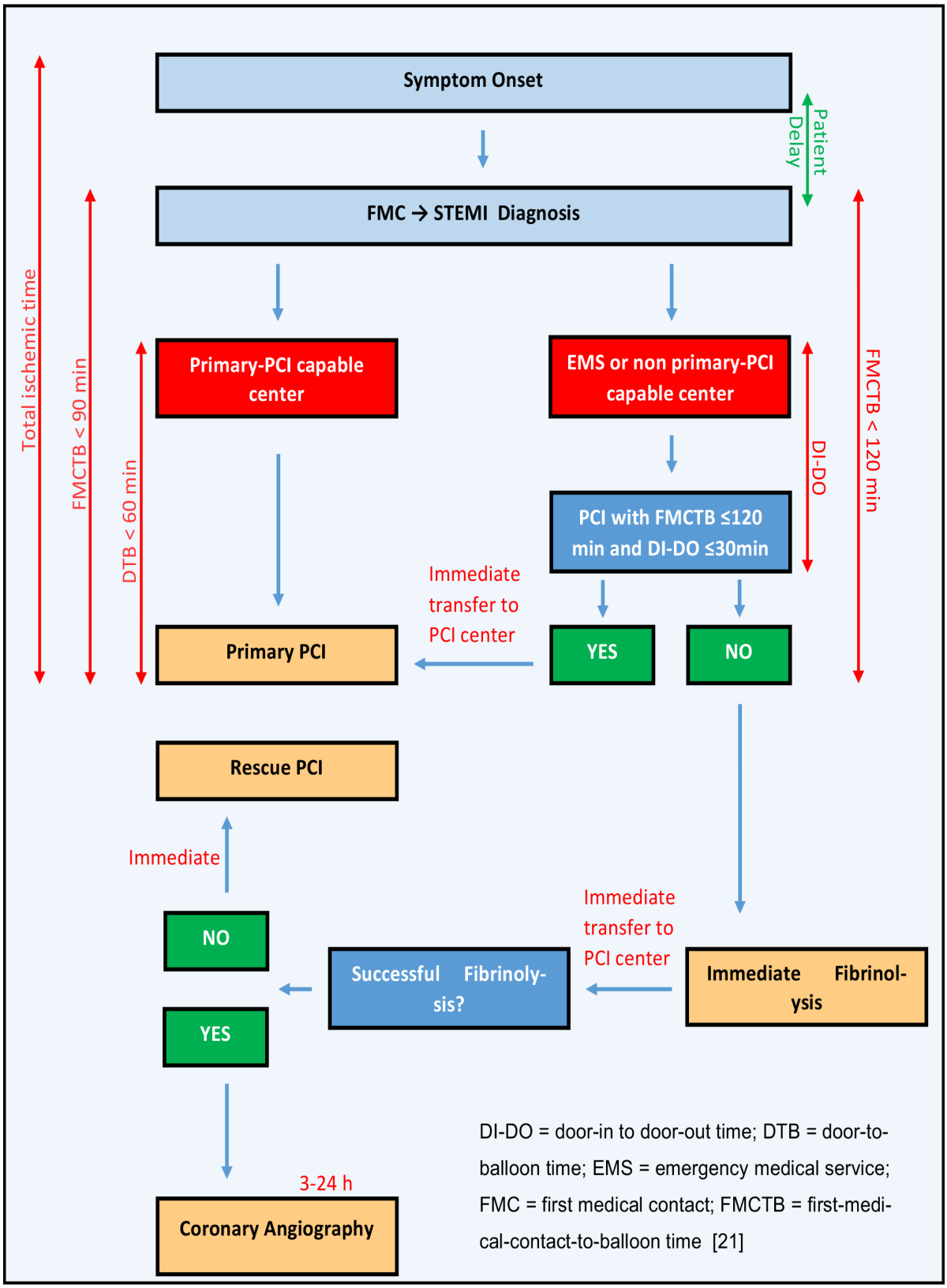

DI-DO = door-in to door-out time; DTB = door-to-balloon time; EMS = emergency medical service; FMC = first medical contact; FMCTB = first-medical-contact-to-balloon time [21]

1.4 Stenting techniques

Lesions in the coronary arteries can develop in every segment of the vascular tree. The location is the crucial factor that determines which kind of stenting technique is applied. In case of a non-ostial and non-bifurcation stenosis, the deployment of a single stent is usually sufficient enough to treat the lesion.

However, it is common that a lesion occurs at a bifurcation, the point where the artery divides into two branches. With a prevalence between 15-20% [22], bifurcations are predilection sites for the development of atherosclerotic plaques, because the division of an artery causes shear stress and hemodynamic turbulence which leads to increased deterioration of the vessel wall. This hemodynamic stress results in the expression of endothelial adhesion molecules and therefor initiates the process of atherosclerotic plaque growth. Because of the fact that these bifurcation lesions are extremely variable in their anatomy (location, plaque burden, angle between branches, size of branches, site of bifurcation), it is not easy to systematically categorize them and it complicates the decision making process for choosing the right stenting method. For a standardized assessment of bifurcation lesions, the classification of Medina et al. proved to be the most popular and intuitive one. In this classification the bifurcation is segmented into three anatomical parts, the main vessel proximal (PMV) of the bifurcation, the distal main vessel (DMV), also referred to as the main branch (MB), and the side branch (SB). Every segment can either be described with 1, meaning that there is a stenosis in excess of >50%, or 0, indicating that there is no significant stenosis. The three figures are separated by commas in this order PMV, DMV, SB. [22–25]

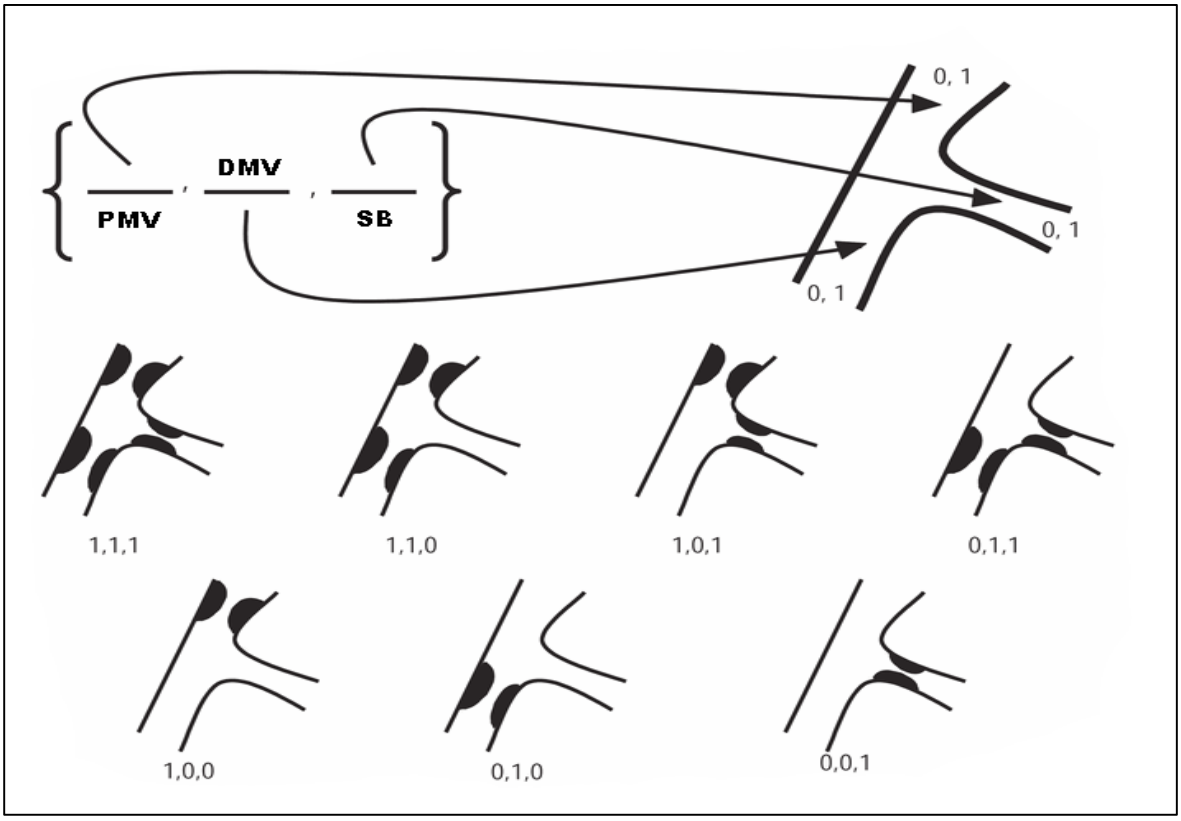

Fig. 3: Medina Classification

PCI of bifurcation disease poses one of the biggest challenges when it comes to coronary stenting. Aside from the numerous combinations of lesions the Medina system already allows, it seems to become an infinite number of possible configurations if we also add the potential angulations of the bifurcation, the size of the main vessel (MV) and the side branch (SB) as well as the different potential morphologies of the lesion like calcification, fibrosis, (non-)ostial and the lesion length. Because of all those mentioned variables, a “one size fits all” solution does not exist for the affected patients but a variety of stenting techniques from which the individually most suitable must be determined. For this reason, another important distinction of bifurcation lesions, namely the division into true (Medina 1,1,1; 0,1,1; 1,0,1) and non-true bifurcation, including all other possible combinations, has to be made. In the latter case, a one-stent strategy should be pursued. For true bifurcation lesions, anatomical characteristics must be considered. [22, 26]

1.4.1 Single stent techniques

T-provisional

The simplest approach is the single-stent technique, among which the T-provisional is the most commonly used method. It consists of the deployment of one stent in the MV across the SB (Fig.4; a), which, if the result is not satisfactory (residual angiographic stenosis >70% after balloon dilatation), can be amended with a second stent deployed in the SB. The stenting of the MV is often combined with the pre-dilatation of the SB in which case a final kissing balloon inflation (FKBI) is recommended (Fig.4; b, see Skirt technique).

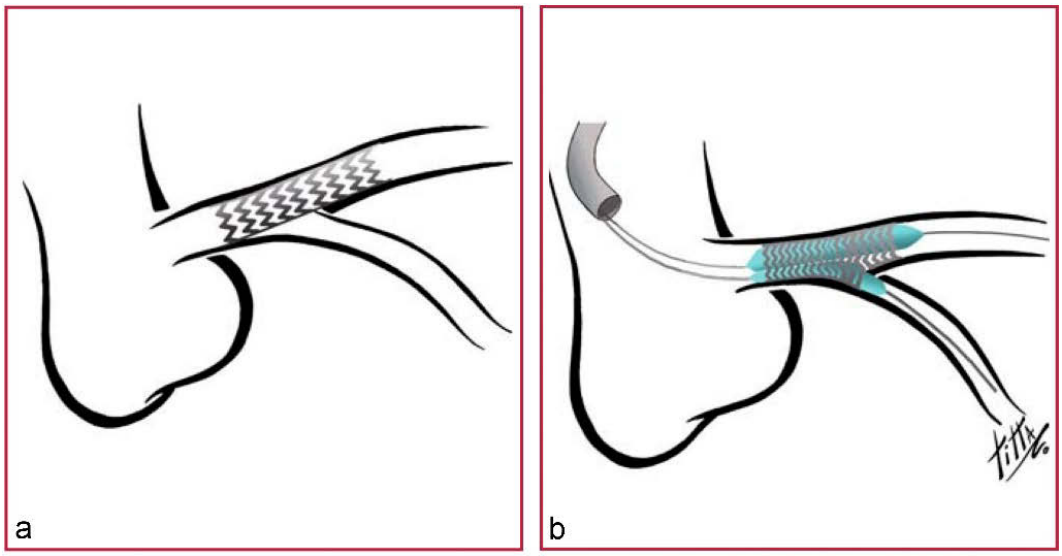

Fig. 4: T-provisional stenting; MV stent (a), FKBI (b)

Skirt

This technique is used if both ostia of the daughter branches are not affected by the lesion and the bifurcation angle is acute. In most cases it is applied at LMCA stenosis without involvement of the LAD and LCX ostia. This method uses one single stent which is placed and unfolded in the MV. Following this, a procedure called final kissing balloon inflation (FKBI) is performed by advancing two guidewires, each with an inflatable balloon at its tip, into both ostia of the daughter branches. Then, they are simultaneously inflated so that they “kiss” at the carina. FKBI modifies the geometry of the implanted stent in a way that it is adjacent to these vessel walls facing the carina of both ostia. The result is a skirt-shaped stent with the widened segment

pointing towards the carina. In case of single-stent placement across the SB, the FBKI is used to crush the stent struts covering the SB ostium and therefore create an orifice without compromising the position of the adjacent stent. Kissing balloon is also an important tool for deploying two stents, one in the MV and another one in the SB, without shifting the carina by inflating only one stent at a time. This also can reduce the risk of MV stent distortion at subsidiary SB stent expansion as well as the likelihood of plaque shift and the compression of the SB, which may already have a narrowed lumen, by the deployment of the MV stent. [27, 28]

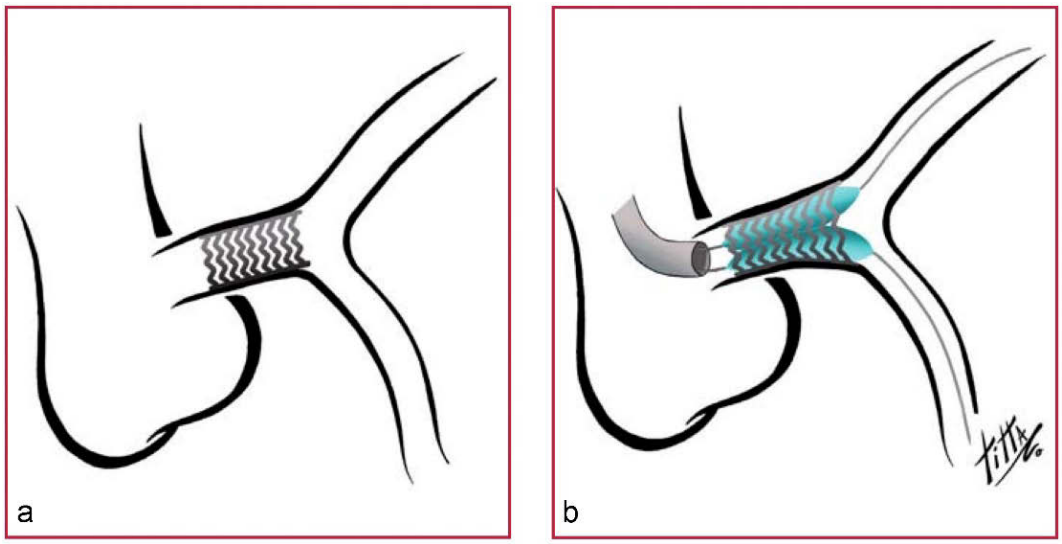

Fig. 5: Skirt technique, PMV stent (a), FKBI (b)

1.4.2 Double stent techniques

Standard and modified T-stenting

The two-stent techniques are required if all three segments of the bifurcation or both daughter branches are diseased. The standard T-stenting is very similar to the T-provisional but that the difference is that a second SB stent is planned a priori. The first stent is positioned in the SB without protruding into the MB. After the stent deployment and the removal of the guidewire and the balloon, the second stent is advanced into the MB. The SB is re-wired and FKBI is performed. The T-modified differs from the standard technique only in the matter that the SB stent is not being deployed until the MB stent is in place.

An important precondition for all T-stenting methods is to have a bifurcation angle

of about 90°. This is necessary for a complete stent coverage of the SB ostium. In case of an acute-angled bifurcation, this technique always leaves an uncovered gap at the proximal part of the SB (Fig.6; b). [27, 29]

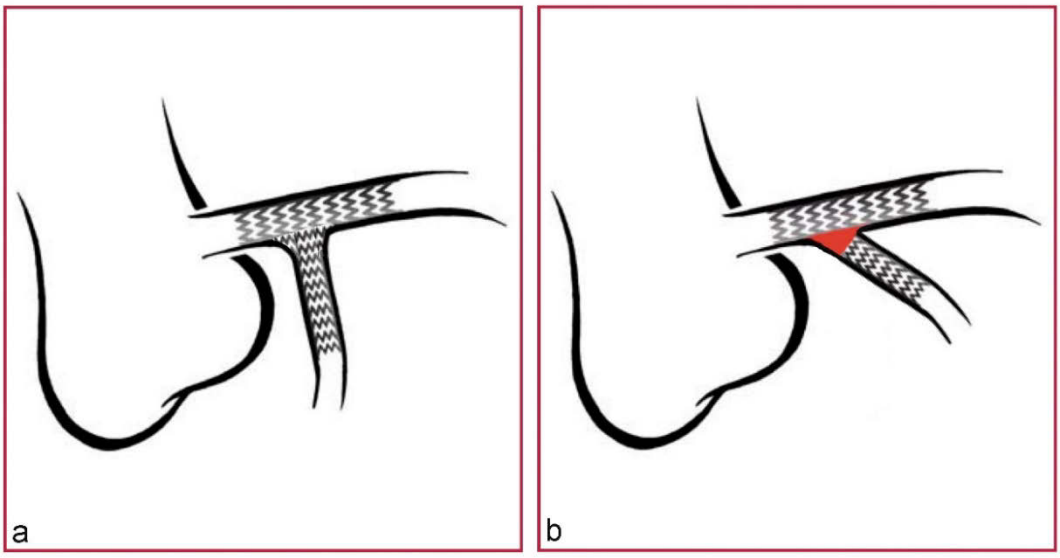

Fig. 6: Standard T-stenting (a) with gap (b)

(Mini-)Crush

The Crush-technique was introduced to avoid the issue of lacking stent coverage at the proximal part of the SB that occurs especially in acute-angled bifurcations. These uncovered gaps turned out to be the most likely cause of restenosis and also significant residual SB stenosis. With this advanced technique it is possible to assure complete coverage of the ostium while having immediate patency of both branches. The procedure consists of placing two stents in the MB and the SB, whereby the former is positioned more proximally than the latter. After the deployment of the SB stent (Fig.7; a), which is intentionally protruding a few millimeters into the MB, the balloon and wire are removed. Hereafter, the stent in the MB is implanted which flattens or so to speak “crushes” the cells of the SB stent (Fig.7; b). The final step is to re-wire both branches and perform a FKBI in order to accomplish the widening of the compressed stent struts that are covering the ostium of the SB without deforming the stent placed in the MB. The downsides of this technique are that the re-crossing procedure for the FKBI can be very laborious and there is still a certain risk of SB restenosis despite the excellent ostial coverage because the

crushing maneuver results in having three layers of metal on just one side of the proximal MB. For this reason, the mini-crush modification evolved, which has the advantage that less stent material is protruding into the MB. [23, 27, 29]

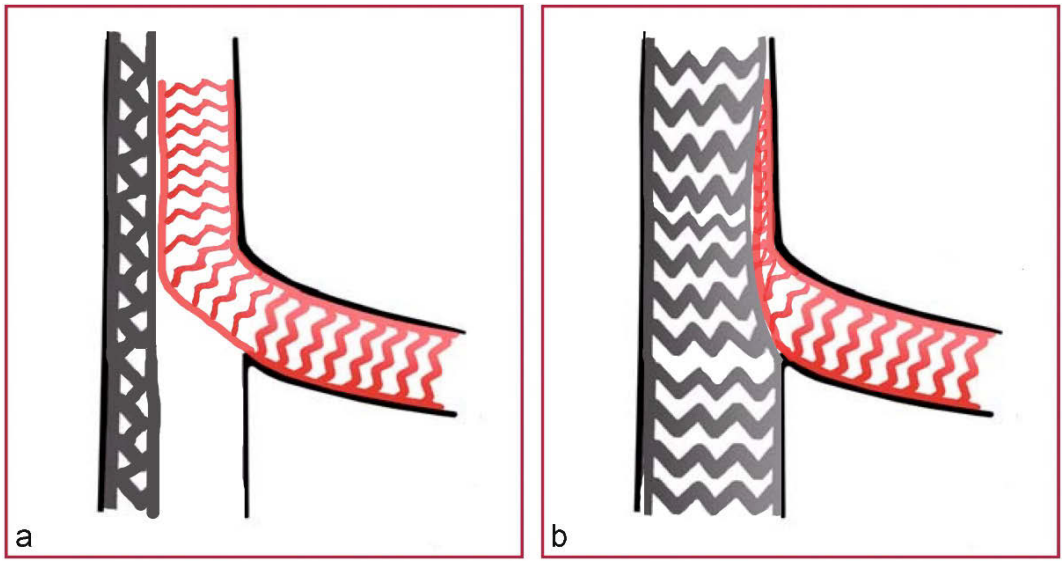

Fig. 7: Crush technique; SB stent protruding into the MV and MV stent is unexpanded (a), Crushing of the SB stent by expanding the MV stent (b)

Culotte

This method is an elegant way to achieve complete coverage of the bifurcation with two stents, but it is necessary that the MV and the SB have approximately the same lumen diameters. After alternating predilatation of both branches, the first stent is deployed in the more angulated branch, usually the SB, which facilitates the following implantation of the second stent. Then, the non-stented branch is re-wired and the struts of the previously implanted stent are dilated by balloon inflation. Through this created opening, a second stent is advanced into the straight branch and deployed in overlap with the first stent in the proximal segment of the MV. FKBI is needed to complete the procedure. The result is a “stent-in-stent” passage in the proximal part of the MV and single stent coverage of the branches. The disadvantages of this technique are that the overlapping stents involve two metal layers adhering to the vessel wall and that incomplete expansion of the inner stent (predisposing: incongruent lumen diameters) could produce a third space between the stents, which both are factors for a potential restenosis. [23, 27, 29]

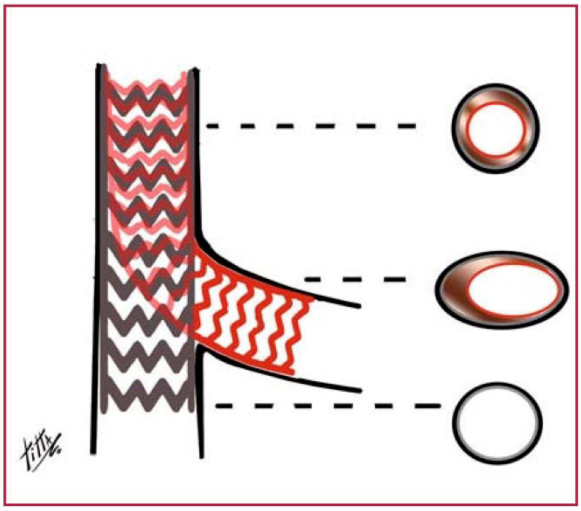

Fig. 8: Culotte technique

V-stenting and Simultaneous kissing stent (SKS)

Both techniques consist of deploying two stents at the same time, one in the MB and the other in the SB. The V-stenting (Fig.9; a) requires a bifurcation angle of less than 70° and it is mainly used if the ostia of both branches are diseased. The simultaneous expansion of both stents, which are not supposed to touch forming a neo-carina, is important to prevent a retrograde shift of the natural carina. In contrast to that, the SKS (Fig.9; b) is used for cases in which the entire bifurcation is affected by the disease and a major difference in lumen diameter of the MV and the branches is presented. Similar to the V-stenting technique, two stents are advanced into the branches but with the difference that they also extend into the proximal MV, where the simultaneous stent deployment results in the formation of a double lumen with a double layer of struts in the center of the vessel. At the point where the two stents touch or “kiss”, a neo-carina is created. The double layer of stent struts and the metallic neo-carina are both risk factors for the development of a thrombosis or a restenosis. Furthermore, the double lumen complicates a subsidiary potential revascularization procedure, for example the placement of a more proximal MV stent without leaving a gap. [27, 29]

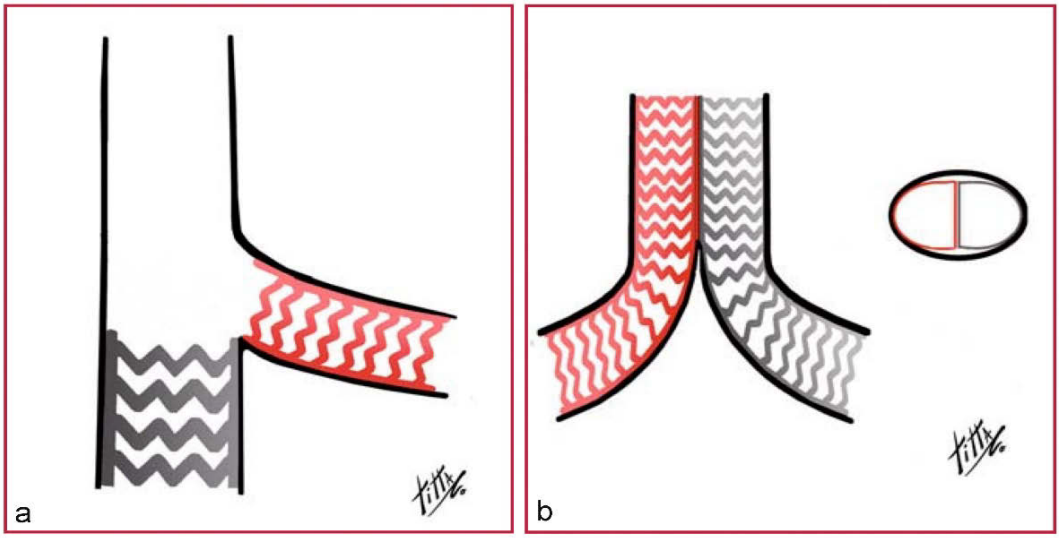

Fig. 9: V-stenting (a) and Simultaneous kissing stent technique (b)

1.4.3 MADS classification

All the techniques mentioned above can be adapted and modified in terms of accomplishing the most suitable result for each patient and the countless anatomical variations. The table in figure 10 shows possible techniques organized by the number of implanted stents, the vascular segment and their chronological order of deployment. This MADS (main, across, distal, side) classification was devised by the European Bifurcation Club. [23]

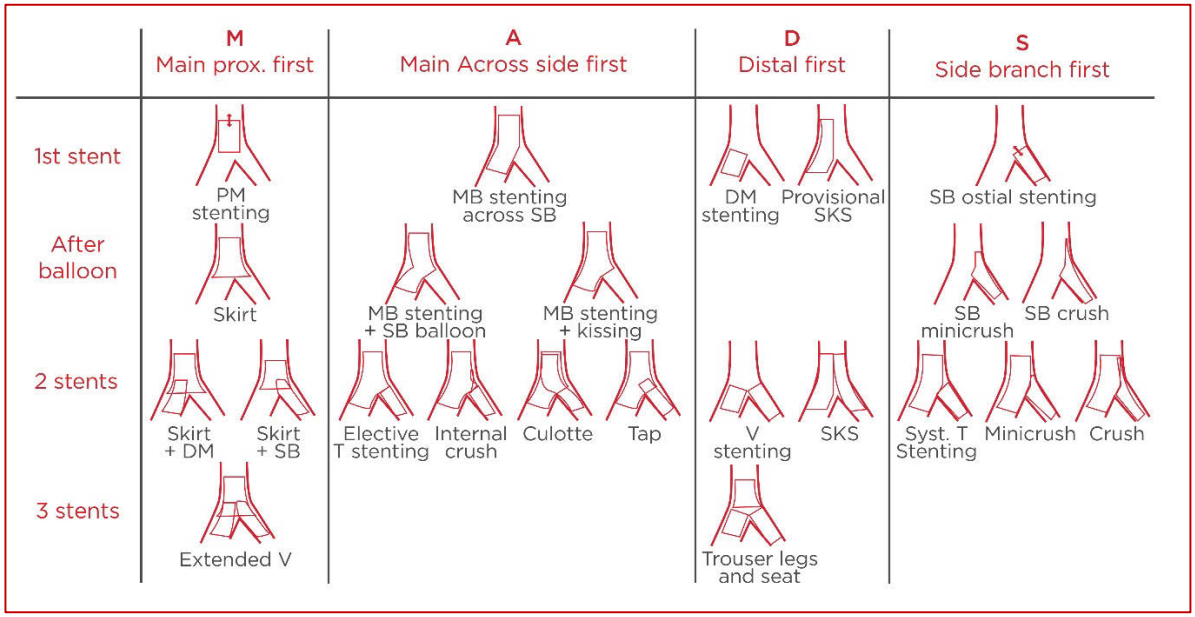

Fig. 10: MADS classification

1.5 Single String stenting technique

The multiplicity of stenting techniques for coronary bifurcation lesions and their continuous development shows that an entirely satisfying solution still has to be discovered. There are two main limitations for all double-stent techniques which are necessary to be resolved. First, there is the superimposition of multiple metal layers, which occurs as a part of the effort to achieve the best possible stent coverage of the diseased vessel wall. It poses a risk for the development of thrombosis and restenosis. Secondly, the incomplete apposition of the stent struts to the vessel wall is sometimes inevitable, because it has to be accepted for the benefit of less stent overlap or better wall coverage. The reason why a completely apposed stent is so important is that DES have the capability of inhibiting the endothelial layers to hypertrophy and therefore minimize in-stent restenosis. However, the drug coated struts can only pursue this function if they are in contact with the endothelium. Moreover, the unintended space between the malapposed stent and the vessel wall causes flow disturbance and exposes even more of the thrombogenic stent surface to the blood stream which may lead to thrombosis. [30–32]

In order to find the technique that combines minimal malapposition, minimal or no overlap of stents and maximal wall coverage, a new approach, called Single String stenting technique, was introduced. It is derived from the “Cross-stenting” technique which Kawasaki et al. reported as a modification of the culotte method.

1.6 Intracoronary optical coherence tomography (OCT)

In the past decade, DES have been increasingly used and the evaluation of their safety has become an important issue. This is because DES have been associated with late stent thrombosis caused by the missing endothelialization of malapposed stent struts. The resulting significance of finding a way to evaluate distances and morphologies in micrometer range led to the introduction of optical coherence tomography for intravascular imaging (IVOCT). IVOCT is an imaging technique that is able to generate high-resolution cross-sectional images by measuring the echo time delay and magnitude of the light that is reflected and backscattered from internal structures in tissue. IVOCT uses near infrared light with wave lengths in the range

of approximately 1000-1300 nm. In contrast to the previously more popular intravascular ultra sound (IVUS), which generates a maximal spatial resolution of 100-200 µm, the IVOCT is capable of achieving an axial resolution of 1-15 µm with a limited penetration depth of up to 3 mm. The lateral resolution ranges between 20-40 µm and is best at the site of the focus. The longitudinal resolution is the product of multiple cross-sectional images recorded while the rotating imaging catheter is being pulled back. The helical type image acquisition is comparable to a spiral-CT, whereby in case of IVOCT, the imaging device is moved and not the sample (patient). The slower the pullback speed or the more frames per second are captured, the better is the longitudinal resolution. [33, 34]

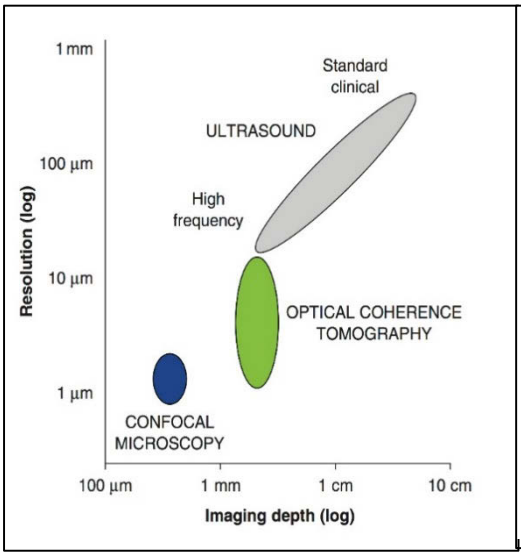

Fig. 11: Resolution and imaging depth of ultrasound vs. OCT

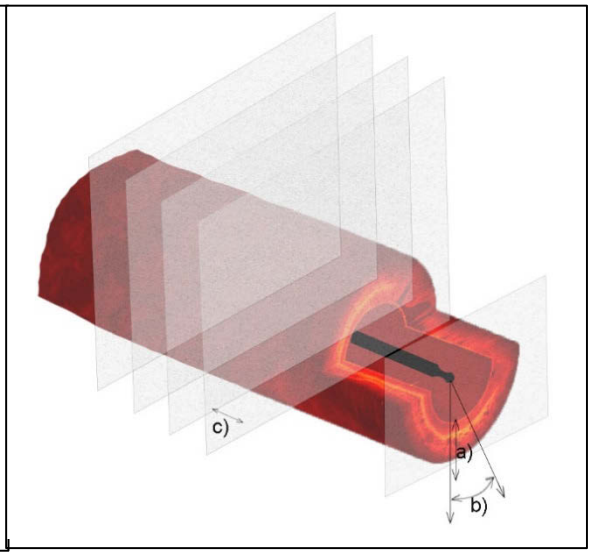

Fig. 12: a)axial, b)lateral, c) longitudinal Resolution of IVOCT

1.6.1 Time domain OCT

Unlike IVUS, which measures the echo time of sound waves that are reflected and backscattered from subsurface structures of tissue to generate the axial resolution, IVOCT measures the echo time of light. This is an important difference because ultrasound is travelling with approximately 1500m/s in water and therefore requires a time resolution of about 100 nanoseconds for the measurement of typical distances with a 100µm scale resolution, which is well within the limits of electronic detection. Light on the other hand travels with approximately 300 000 000 m/s, which would require a time resolution of ~30 femtoseconds (30×10^{-15} seconds) for the measurement of distances with 10µm resolution. Because direct electronic

detection does not work for echo time delays with this speed, a device called interferometer is used.

First generation time domain OCT systems (TD-OCT) were basically modified Michelson interferometers consisting of four main components: light source, reference arm, measurement (sample) arm and detector. The concept of this interferometer is that the emitted light beam travels through a fiberoptic coupler which splits the light beam into two equal portions, one going to the patient via a catheter (sample arm), while the other portion travels a predetermined distance through the reference arm with a defined time delay. A prism at the tip of the fiber optic catheter diffracts the light beam, which has previously been focused by a lens, rectangularly into the tissue. After being reflected and backscattered from the tissue it is collected by the catheter and sent back to the detector to interfere with the returning light from the reference arm. The high-speed photo detector detects the intensity of the interference, which is a pattern of high and low intensities occurring if the distance that both light beams have traveled are roughly equivalent. The axial resolution is determined by the coherence length of the light, whereby low-coherence length results in high-resolution and high contrast images. In order to focus different depths of the tissue with low-coherence light, TD-OCT uses a mechanically moving mirror at the end of the reference arm. Thus, the distances from the sample surface and the reference mirror to the detector are always kept equivalent, which guarantees that the light pulses from both arms coincide and arrive simultaneously at the detector. For the extraction of the echo time measurement, the modulated signal is detected and the extraction of its envelope yields the axial scan (A-scan->A-line). While spinning the speedometer cable and therefore the prism optic at its tip around 360°, multiple A-lines are recorded and composed to a cross-sectional 2D image. The main issue with TD-OCT is that due to the mechanically moving reference mirror, the repetition rate of the A-line scans is limited to a couple of kHz resulting in an imaging speed of only 10-30 frames/s, which makes it unsuitable for fast imaging. This poses a challenge especially for intravascular imaging, because near infrared light is not able to penetrate blood. In order to scan the tissue, the artery has to be blocked or flushed with a contrast agent, both involving a temporary stop of the oxygen supply. In order to minimize the ischemia time during imaging, a second generation of IVOCT systems has been developed. [33–35]

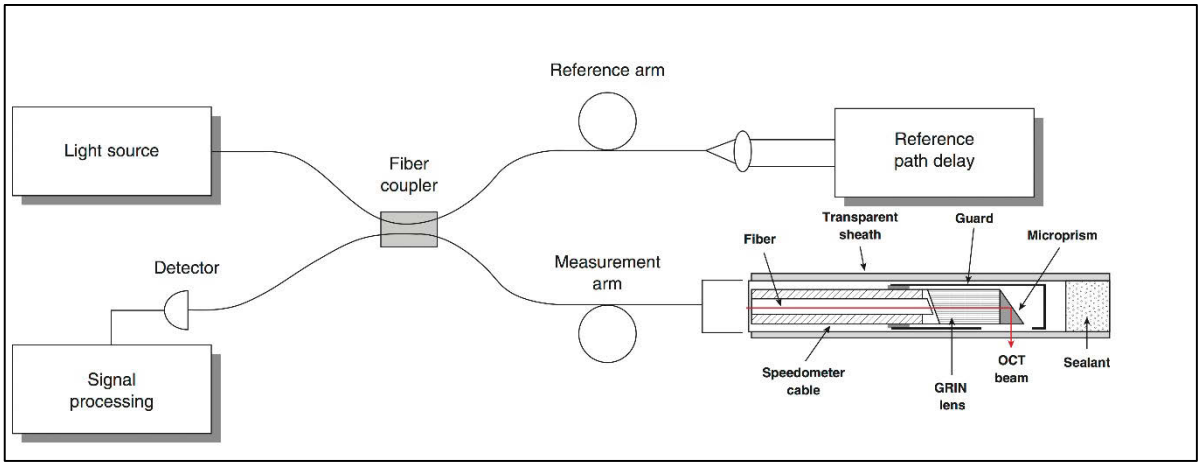

Fig. 13: Schematic diagram of the OCT system

1.6.2 Coronary optical frequency domain imaging (OFDI)

Current optical frequency domain imaging (OFDI) systems use a similar instrumental set-up but they are based on the functional principle of Fourier-domain detection (FD-OCT) providing significant advancements in regard to the image acquisition process and sensitivity. The main difference compared to TD-OCT is that the position of the reference mirror is fixed and a narrow bandwidth light source is used. Each different narrow band frequency of light, generated by a rapidly sweeping laser, is swept as a function of time which leads to a frequency offset of both light echoes, one from the reference and another from the measurement arm. After they have interfered, different frequency modulations are created by different echo delays. The digitalized signal received by the photo detector is then Fourier transformed (mathematical operation) in order to extract the frequency spectrum from the signal and therefore the A-scan. Due to the high-speed swept laser generating a sweep rate up to 200 kHz and the elimination of the mechanically moving mirror, very high frame rates (160 f/s for Terumo Fastview™) are possible, which allows a high longitudinal resolution combined with fast pull-back speeds (20mm/s) and minimized amounts of flushing (contrast-) liquids. [33, 35]

2 Material& Methods

2.1 Study Population

In this trial, 13 Patients eligible for 12 month double anti-platelet therapy and with true bifurcation lesions (Medina 1,0,1 / 0,1,1 / 1,1,1) which involve at least one MB segment plus the SB (extent of SB stenosis ≥ 5 mm) were selected. The mean age was 66,6 years, whereas 9 males and 4 females participated. None of the patients had diabetes but 7 (54%) had a history of hypertension and 10 (77%) presented with hypercholesterolemia. 3 Patients (23%) were smokers and the BMI averaged out at 27,2 percent.

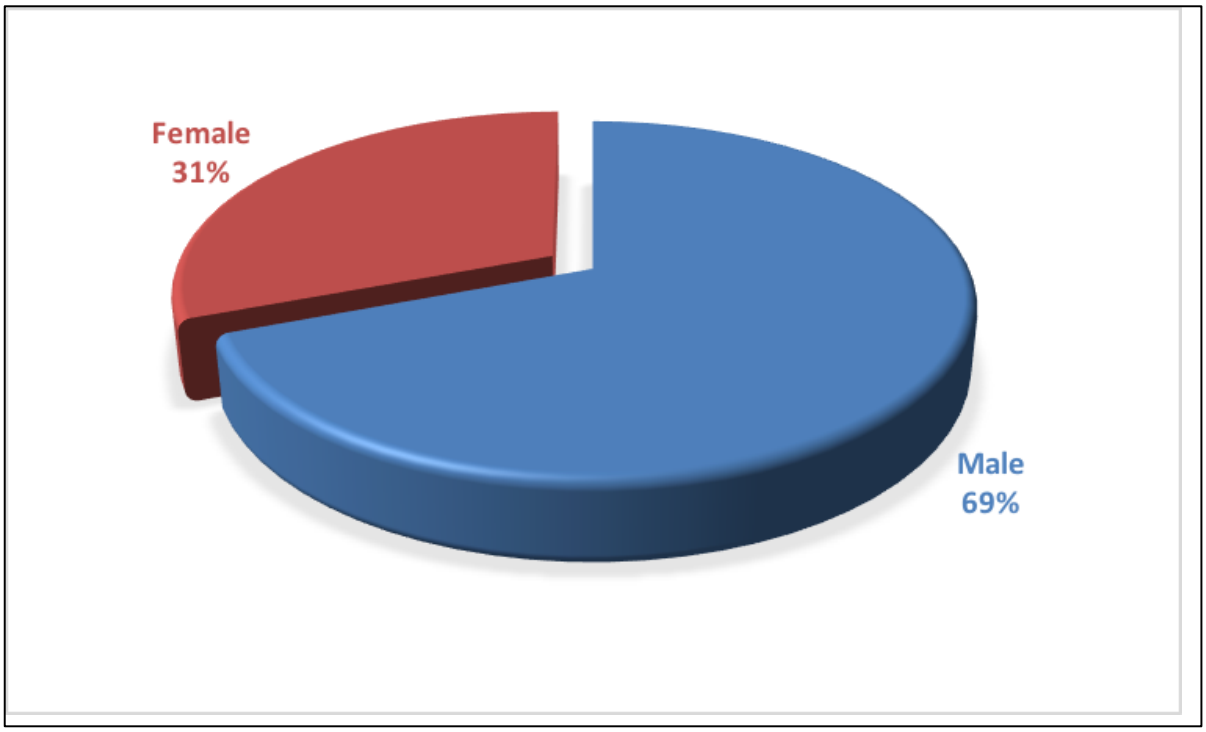

Fig. 14: Gender ratio

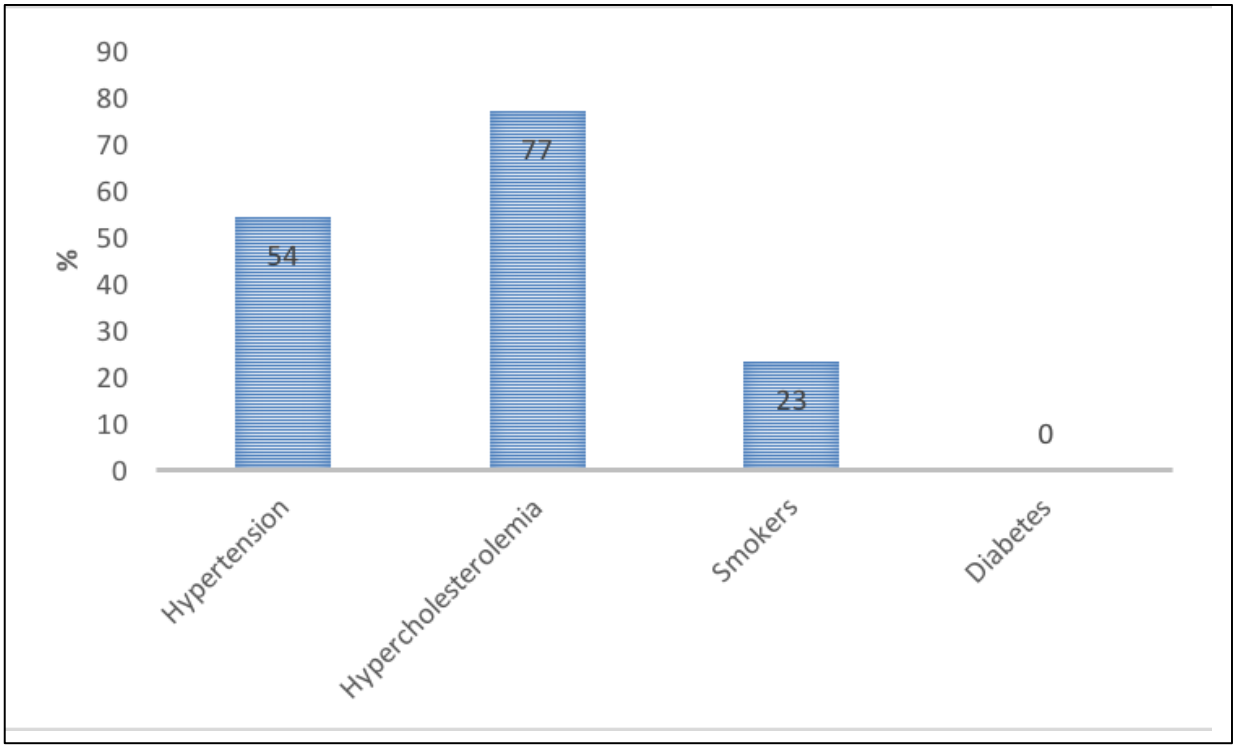

Fig. 15: Risk factor incidence of the study population

2.2 Single String stenting procedure

All single string stenting procedures for this study were performed using uniform materials and a standardized approach. Biomatrix™ and Biomatrix Flex™ drug eluting stents in size of 2.5 mm or 3.0 mm and a maximal cell size of 21.2 or 22.9 mm^2 were deployed. The 120 µm-thick stent struts are covered by a bioresorbable abluminal polymer layer of 10 µm thickness. Two hydrophilic coated guidewires (GW), which in the following are referred to as master and fellow GW, were used. In the beginning, the master GW was advanced into the SB after which the fellow GW was inserted into the distal MB (Fig.11: A). The 2.5 mm SB stent should be carefully positioned with its proximal edge adjacent to the transition point between MB and SB, so that no uncovered gap is created (Fig.11: B). After the deployment (Fig.11: C) with a balloon inflation pressure of 12 bars, the opposite edge of the stent should protrude into the MB no more than one single strut. In order to optimize the proximal position, the balloon was slightly pulled back and reinflated with a higher pressure of 16 bars. The next step is to stir the master GW through the protruding cell, which was performed by pulling it back until it spontaneously falls into this cell (Fig.11: D).

Then, the master GW was advanced through the protruding cell into the distal MB (Fig.11: E) and the crossed cell was dilated using a 2.5 mm balloon (Fig.11: F). Pre-dilatation of the protruding cell may facilitate the re-crossing maneuver. After the positioning of the MB stent through the dilated SB cell (Fig.11: G), the fellow GW was removed which was followed by the deployment of the MB stent. In order to open up the stent struts covering the SB ostium, the master GW was pulled back and rewired into the SB crossing the most distal MB cell facing the ostium. Once this stent cell was pre-dilated using the 2.5 mm balloon, the fellow GW was advanced into the distal MB and FKBI (12 to 12 bars) was performed (Fig.11: H). For further optimization of the proximal MB stent, a 3.5 mm balloon was used to get the the final result (Fig.11: I). [32]

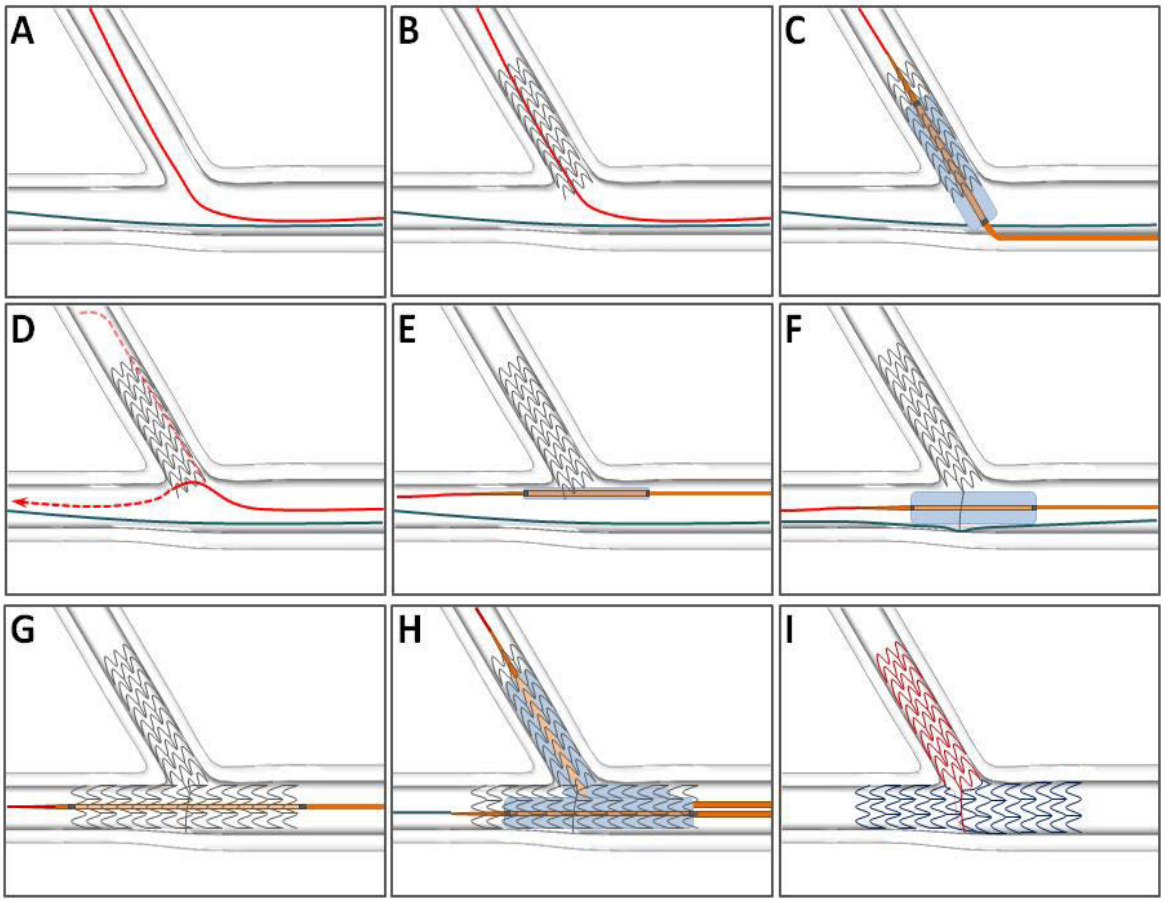

Fig. 16: Schematic sequence of Single String stenting procedure; master-guidewire (red),fellow-guidewire (blue); see detailed information in the main text

2.3 OFDI acquisition of bifurcation lesions

OFDI was performed systematically on all eligible patients before and after single string stenting. Image acquisition parameters were adjusted with the Terumo Lunawave console and pullback runs with the speed of 20 mm/s were performed using a radiopaque Terumo Fastview catheter with a maximal pullback length of 150 mm. The Fastview catheter, equipped with the imaging element rotating at 9600 rpm, provides a frame acquisition rate of 160 f/s. It was advanced over a standard 0.014 in GW into the eligible left coronary segment. After crossing the lesion and positioning the catheter at the distal end of the stenosis, a pullback run was performed during automatic continuous intracoronary injection of 100% contrast medium (Visipaque™=Iodixanol) with a flow rate of 3-4 ml/s at the maximum of 4 seconds. Four pullback runs were performed per patient, one before plus another after stent deployment, always in the distal MB as well as in the SB, both extending into the proximal MB.

2.4 Image analysis

The image analysis was performed using the Terumo Lunawave console. For the analysis of the stent strut apposition, the post-interventional runs of each bifurcation lesion, including main- and side branch (if it was available), were selected. For reasons of comprehensibility and better arrangement, the bifurcation was separated into five anatomical segments. The proximal MB (pMB) extends to the proximal SB ostium. The MB bifurcation area (B-MB) corresponds to the part of the MB facing the SB ostium, which is additionally divided into an abostial as well as an ostial 180 degrees. The third segment is the distal MB (dMB) starting at the carina. The bifurcation area, where the SB truncates into the MB (B-SB) and the area distal of it (dSB), where the SB lumen returns to being circular, are the two segments of the SB (see Figure 14). The distances of the stent struts were measured in the 2D cross-section images whereas frame by frame (distance between frames: 0,1 mm) analysis was performed in the B-MB and the B-SB segment. In each of the three remaining segments (pMB, dMB, dSB), five adjacent frames with a 1mm interval were analyzed.

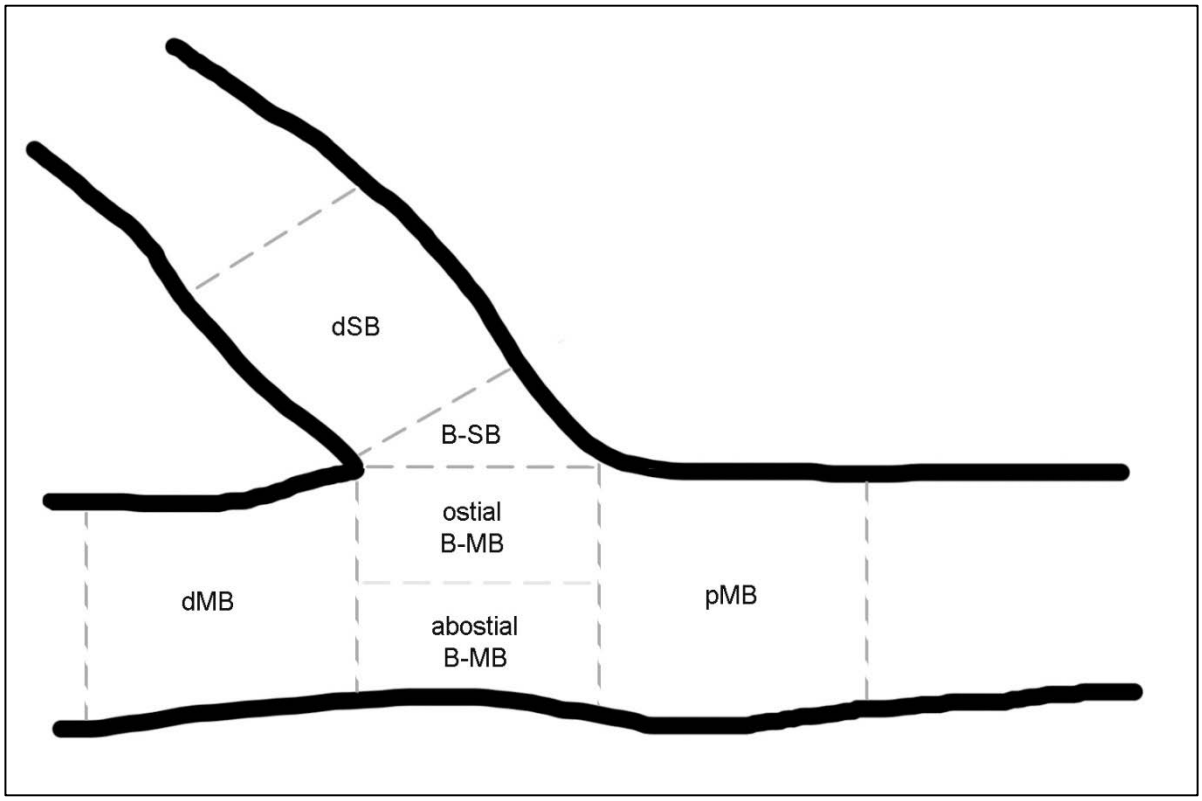

Fig. 17: Bifurcation segments

After the patient's image data is loaded into the measurement program, the first step is to calibrate the Z-offset by manually adjusting the catheter diameter so it is adjacent to at least three of the four quadratically arranged lines (Figure 15: green arrow). This ensures the fidelity of the spatial representation of the image, which is required for accurate measurements. Following this, the distal part of the SB ostium (carina; Figure 16: green arrows) has to be located in the longitudinal image in order to get the cross sectional image of the vessel at this position. Then, the image is rotated until the SB ostium is pointing towards 12 o' clock (Figure 16: yellow star), which is necessary for an easier distinction of the ostial and abostial 180 degrees. After these adjustments the actual distance measurements of the stent struts are performed. For this purpose, the image is magnified by the factor of 2.45x, which facilitates accurate measuring while giving enough overall view to detect shadows and reflections from the struts. Generally, there are two characteristic features to identify the metallic stent struts. For one, there is the bright hyperdense reflection (Figure 15: red arrow) and secondly, the shadow (Figure 15: white arrow) caused by the metal struts that are not penetrable for the OCT light beams, whereas one of

these features is sufficient for the strut identification [36]. Depending on the angle the light beam impinges on the strut and the sectional plane, the shadow and the reflection can be absent or attenuated. The distances between the vessel wall and the stent struts were obtained in a clockwise order starting at 9 o'clock until 3 o'clock for the ostial 180 degrees and from 3 to 9 for the abostial semicircle (Figure 17). The distances were always measured from the center of the strut's lumen-facing surface to the closest point of the arterial wall. Because of the shadow associated to the strut and the resulting signal cancellation, the vessel wall is sometimes not differentiable in the area behind the strut with the consequence of having to extrapolate the spot where the shortest distance to the vessel outline is expected. The Terumo software only allows a total amount of six measurements in each cross-sectional image, which is mostly insufficient. In order to avoid this restriction, the distance values have to be transferred into an Excel chart after every six measurements and cleared in the Terumo program in order to measure six new distances. This analyzing process was repeated for multiple cross-sectional images in the above mentioned pattern using frame by frame or 1mm interval steps. All previously performed measurements and their resulting distances were filled in an Excel sheet, whereas each patient was analyzed separately. Every sheet was organized following the pattern of the bifurcation segments described in figure 15, starting with the distal main branch, ostial and abostial main branch bifurcation, proximal main branch, side branch truncating into the main branch and distal side branch. The cross-sectional frames were arranged horizontally with the values for all stent struts in the corresponding frame listed in columns below. In 8 out of 13 cases, there was no OFDI data from the side branch available so that only the main branch was evaluated.

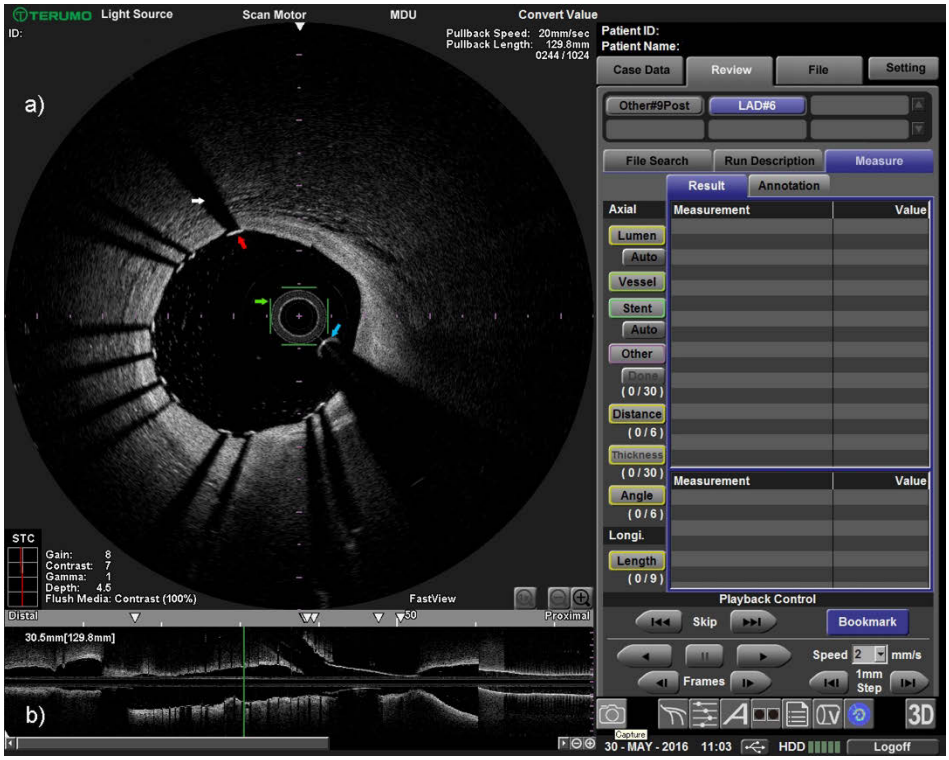

Fig. 18: a) Cross-sectional image with stent strut (red arrow), strut shadow (white arrow), Z-offset calibration bars (green arrow) and guidewire (blue arrow); b) longitudinal view with the green indicator line for the position of the cross-sectional image

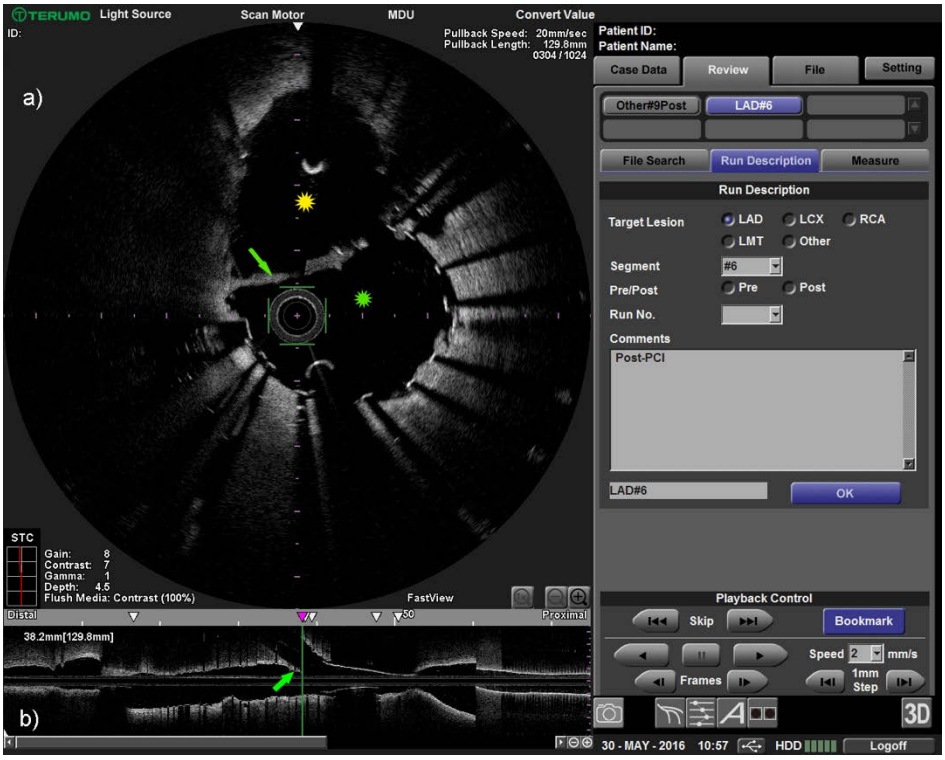

Fig. 19: Carina (green arrows), MB lumen (green star) and SB lumen (yellow star)

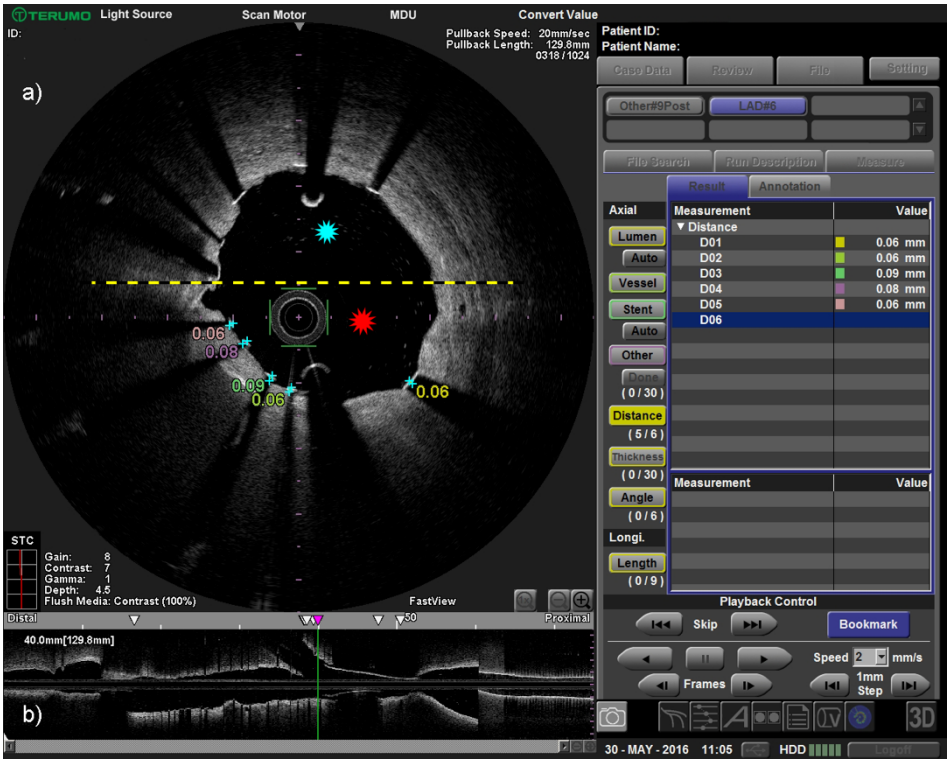

Fig. 20: Ostial lumen (blue star) and abostial lumen (red star) with distance measurements

2.5 Statistical Evaluation

The statistical evaluation was conducted using Microsoft Excel. Each patient was analyzed separately in regard to the following target values:

1) Absolut number and percentage for stent struts with perfect apposition
   ➔ Distance between vessel wall and stent strut = 0 µm
2) Absolut number and percentage for stent struts with marked malapposition
   ➔ Distance between vessel wall and stent strut > 200 µm

Because of the fact that all distances were measured from the luminal side of the stent strut to the vessel wall, the thickness of the strut and its drug covered layer, which together add up to 90 µm, have to be subtracted from the original value in order to get the actual vessel wall-strut-distance. After this adjustment, both target values were determined for all six bifurcation segments, four, if no side branch data was available. After the summation of these partial results and the calculation of the

exact percentage of perfectly apposed and malapposed stent struts, the results for each patient were entered into a final table.

3 Results

All 13 in vivo procedures were successfully performed according to the protocol, whereas only in five cases, the complete data of two post-interventional OFDI pull-back runs, namely the MB and the SB run, were available. Regarding the other eight cases, only the MB but not the SB could be analyzed. The reason for the missing SB data was either the unfeasibility of the OFDI procedure itself during the PCI or the not analyzable image information due to severe artefacts or incomplete pullback. In all 13 cases, a total number of 465 OCT frames was analyzed and 6370 stent struts were identified for evaluation. All six bifurcation segments considered, an overall number of 3405 stent struts (67%) showed perfect apposition (=0 µm), whereas marked malapposition (>200µm) was seen in 406 struts (8%). 1280 struts (25%) were in the not additionally defined range between 0 and 200 µm (0<X<=200).

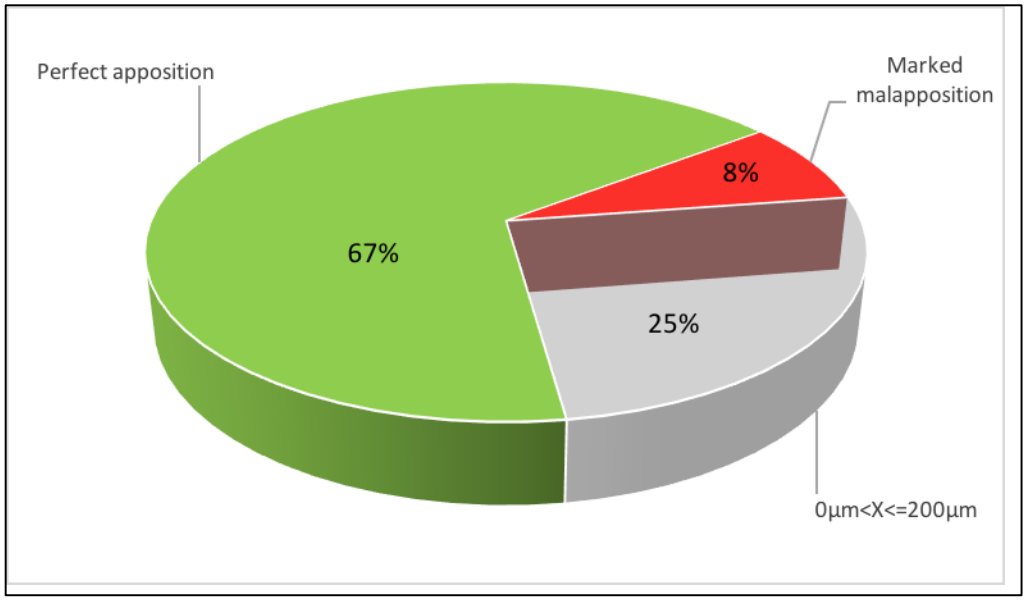

Fig. 21: Diagram of the percentage distribution

The detailed evaluation of the important bifurcation segments (see Figure 15) ostial B-MB and abostial B-MB yielded perfect apposition in 1665 struts (59%) and marked malapposition in 329 struts (12%). In five cases, where SB data was available, the B-SB area showed perfect apposition in 480 struts (71%) and marked malapposition in 50 struts (7%). Limited evaluation of the segments dMB and pMB showed perfect apposition in 1060 struts (79%) and 26 (2%) were seen as marked malapposed. In case of the remaining dSB area, 200 struts (87%) were perfectly apposed and one strut (<1%) was malapposed.

Per-case stratification yielded a rate of perfect apposition of 65.8 ± 16.0% and a rate of 8.2 ± 6.8% for the marked malapposition.

Rate of apposition, %	p/a	m/m
Total bifurcation segments	65.8 ± 16.0	8.2 ± 6.8
pMB	73.6 ± 16.8	2.9 ± 3.5
dMB	79.7 ± 23.4	1.0 ± 2.1
ostial B-MB	61.3 ± 22.1	13.7 ± 10.4
abostial B-MB	61,1 ± 27.2	6.9 ± 11.0
B-SB	70.3 ± 16.2	8.0 ± 6.2
dSB	85.9 ± 6.2	0.4 ± 0.8

Fig. 22: Rate of apposition (mean ± SD) in bifurcation segments; perfect apposition (p/a) and marked malapposition (m/m)

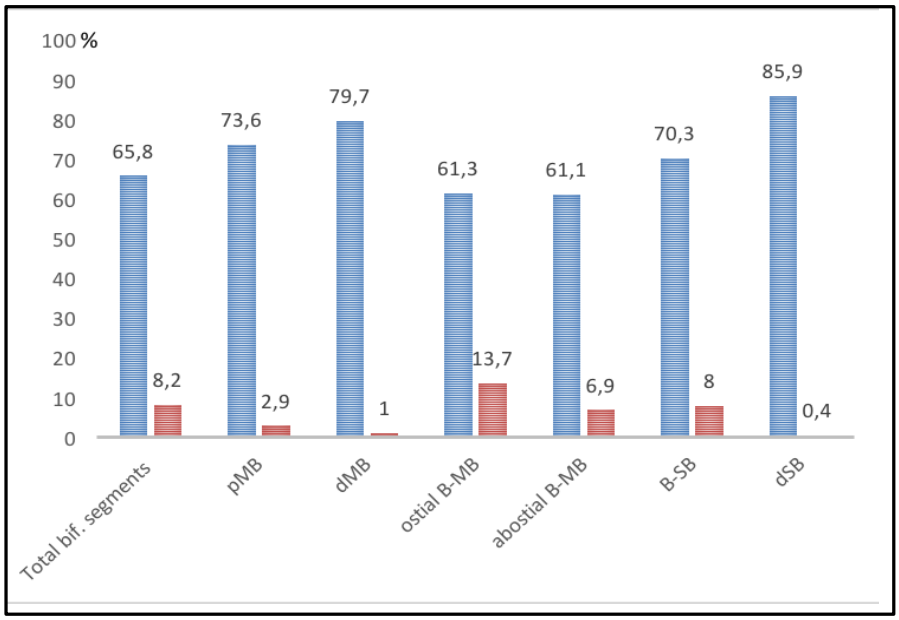

Fig. 23: Percentages of perfect apposition (blue) and marked malapposition (red)

4 Discussion

This study is based on the findings and presumptions Toth et al. [32] made in their proof-of-concept study for in vitro single string stenting of coronary bifurcation lesions. The ambition was, to confirm the in vivo feasibility of this new technique as well as its superiority towards conventional two-stent techniques regarding the rate of stent strut apposition. In general it was shown that the single string technique is perfectly applicable for bifurcation lesions in humans. The concept of this approach supported by the analysis of the in vitro data already hinted at being superior to many, if not all, double-stent techniques because of the following reasons which were stated by Toth et al. (34):

1. Overlap of stents is minimized to 1 single ring. However, it is important to realize that in case of extremely shallow angulations, the protrusion might be up to 2 cells, resulting in double-strut overlap. Compared with other conventionally applied techniques (culotte, crush, mini-crush), this level of overlap is still minimal. that in case of extremely shallow angulations, the protrusion might be up to 2 cells, resulting in double-strut overlap. Compared with other conventionally applied techniques (culotte, crush, mini-crush), this level of overlap is still minimal.

2. Because the SB stent is literally pulled toward the MB while inflating the balloon in the single string, this portends optimal and full coverage of the SB ostium and the carina (unlike T-stenting and pro- visional T-stenting) .

3. Malapposition and neocarina formation is minimal (unlike T- and Protrusion stenting or kissing stent).

4. The single string technique is applicable for any size vessel, as well as any extent of atherosclerotic plaque (unlike dedicated devices).

5. The single string technique can theoretically be applied with any commercially available conventional stent, with sufficiently large cell designs, even though specific design features may offer better solutions than others.

Although the hypotheses of the items one and two can not be validated by this study because it would require a 3-dimensional reconstruction and structural analysis of the OCT image data, all segments but especially the bifurcation area (B-MB, B-SB) showed a favorable rate of malapposition. As far as the study population of this trial is concerned, the single string stenting was applicable for all patients, no matter what the size of the vessel or the extent of atherosclerotic plaque was. Furthermore, any conventional stent with sufficiently large enough cell design can be used with this new technique.

The results of the in vitro tests that Toth et al. conducted showed an overall rate of perfect apposition of 83.0 $\pm$ 9.2% (see Figure 25). The rate of stent struts with marked malapposition was 4.4 $\pm$ 5.3%. Compared to the above mentioned results of the in vivo procedures (p/a: 65.8 $\pm$ 16.0%; m/m: 8.2 $\pm$ 6.8%), the percentage of malapposed stent struts is nearly twice as high as it is in vitro. Moreover, the in vitro apposition rate is about 20% higher than the results of the in vivo stenting. Both numbers confirm, that the in vitro findings can not simply be turned into a one-on-one comparison for in vivo procedures. It shows that there are too many unpredictable anatomical variables and pathologies like bifurcation angulation, vessel caliber or disease distribution, which can not be simulated in phantoms. Nonetheless, results from multiple in vivo and in vitro studies investigating the malapposition rate within the bifurcation area for various stenting techniques were in the range of 30-45%. Compared to the results of the single string stenting technique with malapposition rates of 13.7$\pm$ 10.4% (abostial B-MB), 6.9 $\pm$ 11.0% (ostial B-MB) and 8.0 $\pm$ 6.2% (B-SB), this new approach shows a promising benefit for the critical bifurcation area. [32]

Optical Coherence Tomography-Derived Data			
Rate of malapposition, %	f/a	m/m	Floating
Total bifurcation areas*	83.0 ± 9.2	4.4 ± 5.3	1.6 ± 3.3
Proximal: ostial*	77.0 ± 16.0	4.7 ± 12.0	1.0 ± 3.3
Proximal: abostial*	94.0 ± 6.6	1.6 ± 2.1	0.1 ± 0.4
Distal: ostial*	59.0 ± 26.0	16.0 ± 19.0	6.3 ± 11.0
Distal: abostial*	87.0 ± 11.0	0.8 ± 1.6	0.1 ± 0.4
Side branch: abostial*	94.0 ± 7.3	0.8 ± 2.2	0.3 ± 0.8

Values are mean ± SD. Overview of the main branch and side branch ostial area obstruction and string angle (analyzed by micro computed tomography) and the overall rate of malapposition in the bifurcation and in the different areas of the bifurcation separately (analyzed by optical coherence tomography). In the latter, the struts are categorized as fully apposed struts in which the distance between the strut and the phantoms wall is practically 0, markedly malapposed struts (malapposition >200 μm), and floating struts (malapposition >500 μm). *Total bifurcation: areas 2/3/4/5/6; proximal ostial, area 2; proximal abostial, area 3; distal ostial, area 4; distal abostial, area 5; side branch abostial, area 6.

f/a = full apposition; m/m = marked malapposition.

Fig. 24: Toth et al. in vitro study; Rate of apposition in bifurcation segments; perfect apposition (f/a) and marked malapposition (m/m)

4.1 Comparison to other studies

Tyczynski et al. [37] conducted a study in order to assess the malapposition rate of simple stenting techniques compared to more complex techniques, i.e. Culotte's. They evaluated the OCT images of 14 patients that had been treated with the said stenting technique and they found a median malapposition of 50.3% for the ostial B-MB segment (toward SB) and 14.2% for the abostial B-MB segment (opposite SB). The single string stenting technique on the other hand showed a median malapposition of 12.1% for the ostial B-MB segment and 0.6% for the abostial B-MB segment. Besides the lower malapposition rate of the bifurcation area, the pMB and dMB segments show favorable results in case of single string stenting as well. Due to the similar size of the study population and an equivalent retrospective design, good comparability between their results and those showed in this thesis is given. Nevertheless, there is a difference in the way of defining the distance which identifies a strut as malapposed. While Tyczynski et al. diagnosed a malapposed stent if

the distance was > 0 µm with a error margin of 15 µm, we set the threshold value to >200µm in order to rule out measurement inaccuracies. This implicates, that our rate of malapposition are lower but with the advantage of having more certainty that the malapposition is absolute. In order to show a significant reduction of the malapposition rate and therefore the superiority of the single string stenting procedure, a comparative trial with equal benchmarks is necessary.[37]

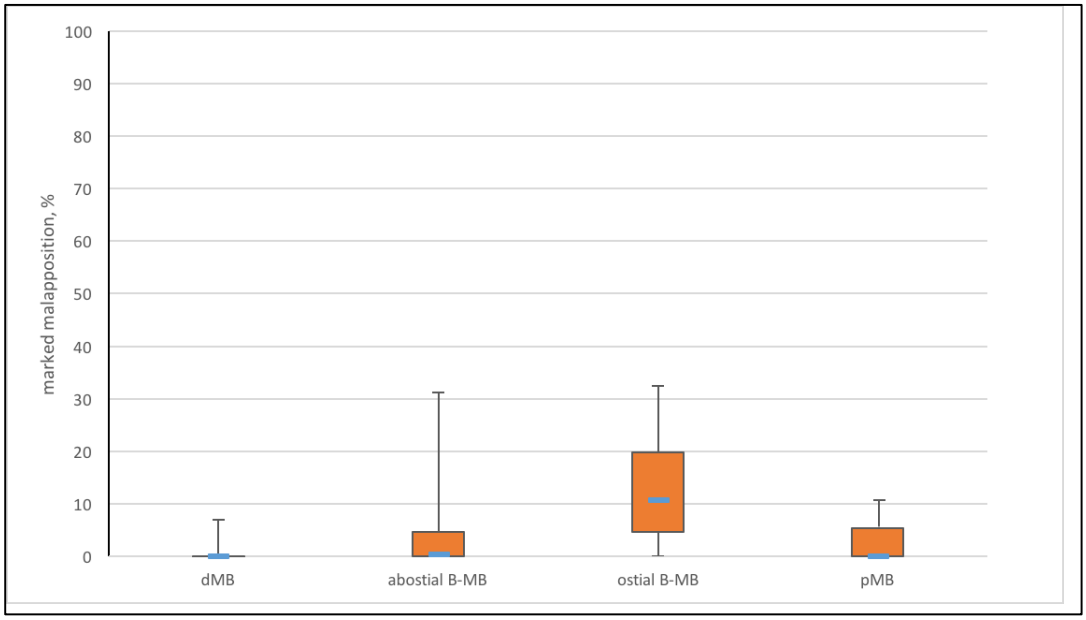

Fig. 25: Malapposition rates for single string technique over 4 segments

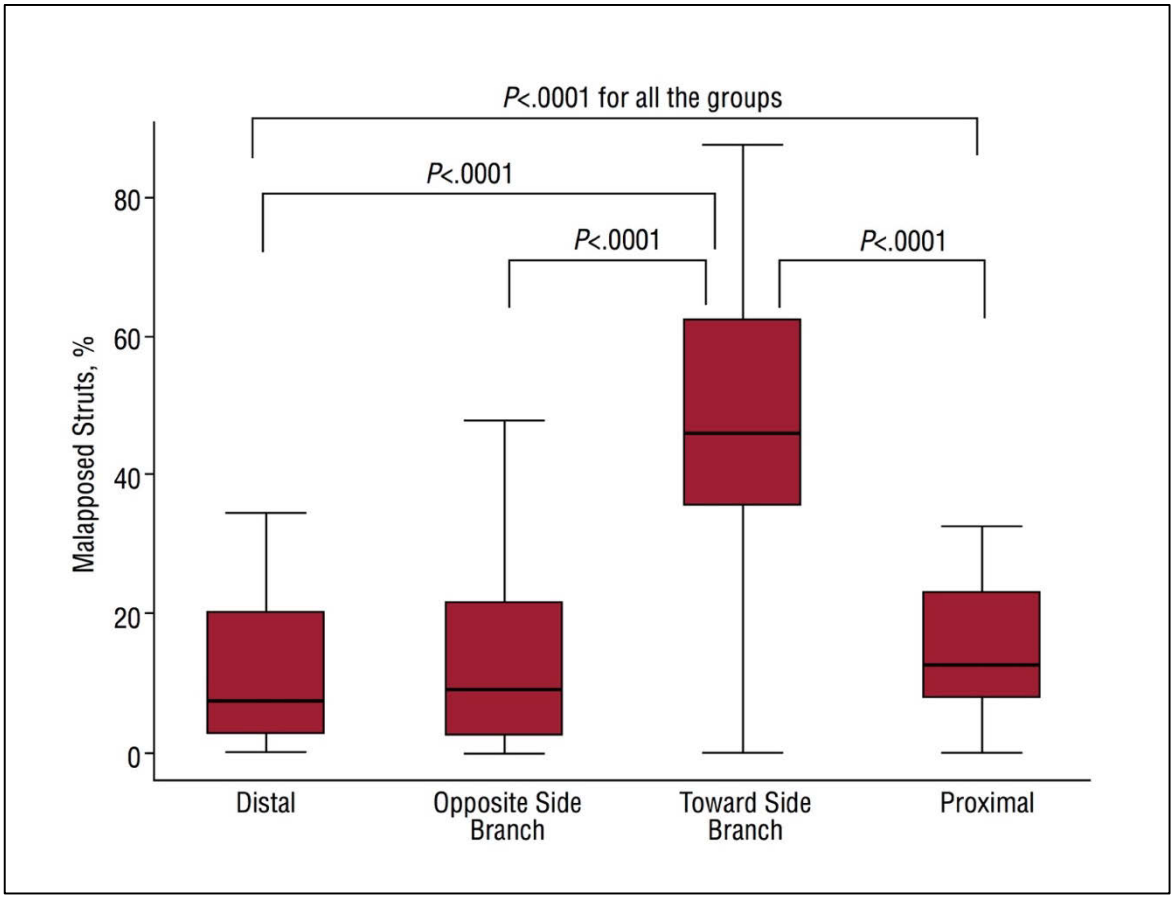

Fig. 26: Malapposition rates for Culotte's technique over 4 segments

(dMB=Distal, abostial B-MB=Opposite Side Branch, ostial B-MB=Toward Side Branch, pMB=Proximal)

Foin et al. also assessed the rate of malapposed stent struts for the deployment of one MB stent and consequential FKBI in models of a coronary bifurcation. They analyzed the results of the stent deployment (n=42) using high-resolution micro computed tomography. In their study, they set the threshold value for the definition of a malapposed strut to >150µm. The analysis of their stent strut-vessel wall distances yielded an average rate of malapposition in the bifurcation area of 20.2 ± 6.4% (vs. 10.3 ± 11.3% in single string) and 26.0 ± 5.7% toward the SB ostium (vs. 13.7 ± 10.4% in single string). Despite the fact of optimal in vitro conditions, they attained a malapposition rate approximately twice a high as the in vivo procedures of the single string stenting technique. [38]

4.2 Limitations

Due to the relatively small number of patients included in this trial, the variance of the results for the by-case analysis is notable. Especially one Patient showed above-average deviations from the mean malapposition rate of up to 35% and below-average deviations from the mean apposition rate of up 55%. As a consequence, the values of the standard deviation are up to 27.2% (see Figure 28). In order to minimize the problem of above-average aberrations and to increase the accuracy, future study populations have to be enlarged.

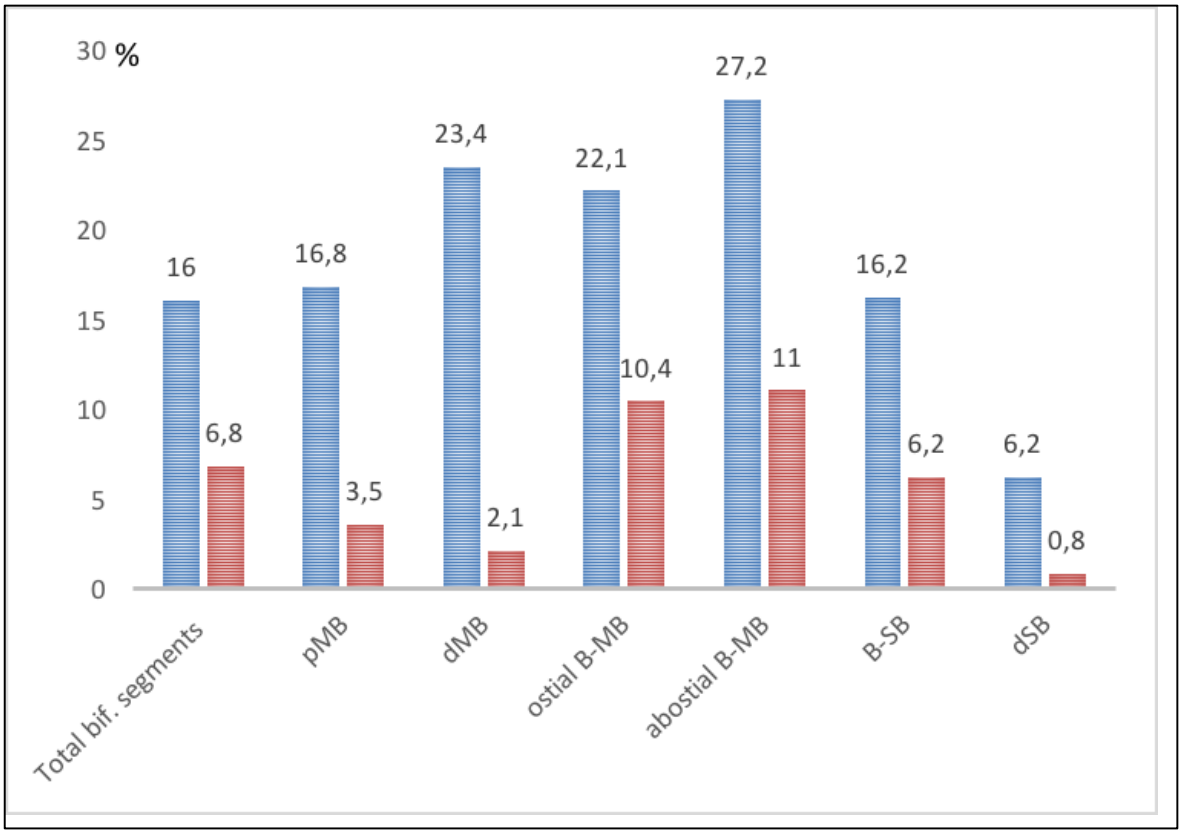

Fig. 27: Standard deviations (%) of the bifurcation segments; perfect apposition (blue) and malapposition (red)

Another limitation is that a direct comparison between the patient's outcome at single string stenting and the outcome of the same patient if he had been treated with a conventional stenting technique, is not possible. Furthermore, the long term follow-up regarding the presence of restenosis or in-stent thrombosis was not taken into consideration and was beyond the scope of this thesis, even though there is no reason to expect a difference compared to other double-stent techniques. Because of the lack of data regarding the bifurcation segments of the side branch (B-SB, dSB), only 5 patients could be analyzed in this matter. This means that the results from the segments B-SB and dSB are not 100% comparable to the other four segments (with data from 13 patients) because of the larger statistical error based on a smaller study population and therefore a larger impact of the deviating values. Especially regarding the comparability of the B-SB segment and the important B-MB segment, the results have to be seen under reserve.

4.3 Conclusions

In this study the feasibility of the single string stenting approach was clearly demonstrated. The procedure was applicable for all participating patients and for this technique, there are basically no limitations regarding the type of stent or the manufacturer. In general, the rates of malapposition this trail yielded are favorable, even if the comparability with the result of other double-stent techniques are not fully possible, due to deviating measurement techniques and the different definition of the target values. At this point, there is no further prediction regarding other important factors like wall coverage and stent overlap possible.

4.4 Perspective

Although this study showed promising results regarding the apposition rates for single string stenting of coronary bifurcation lesions, the application of this technique and its advantages need to undergo further in vivo testing in order to confirm and specify the results of this trial in a larger study population. Moreover, future studies have to investigate additional issues like strut distortion, vessel-wall coverage, MB

and SB openings at the ostium, crossing of the most proximal stent cell, intact SB angulation and post-procedural anatomy, which were beyond the scope of this thesis. In order to be able to draw a final conclusion about the superiority of single string stenting towards other double-stent techniques, a comparative clinical trial with an equal study size and matching study parameter will be necessary.

5 Appendix

5.1 References

1. Coronary Artery Atherosclerosis: Practice Essentials, Background, Anatomy. 17.09.2015. http://emedicine.medscape.com/article/153647-overview#showall. Accessed 30 Sep 2015.
2. Aaron. CV Physiology: Coronary Artery Disease. 21.07.2015. http://www.cvphysiology.com/CAD/CAD001.htm. Accessed 30 Sep 2015.
3. Angela Pirillo, Giuseppe Danilo Norata, Alberico Luigi Catapano. LOX-1, OxLDL, and Atherosclerosis. Mediators of Inflammation 2013;2013:1–12. doi:10.1155/2013/152786.
4. Singh Raja B, Mengi Sushma A, Xu Yan-Jun, Arneja Amarjit S, Dhalla Naranjan S. Pathogenesis of atherosclerosis: A multifactorial process. Exp Clin Cardiol 2002;7:40–53.
5. Roberts WC. The cause of atherosclerosis. Nutr Clin Pract 2008;23:464–7. doi:10.1177/0884533608324586.
6. Willerson JT, Holmes DR, editors. Coronary Artery Disease. s.l.: Springer-Verlag; 2015.
7. Frink RJ. Inflammatory atherosclerosis: Characteristics of the injurious agent. Sacramento, Calif.: Heart Research Foundation; 2002.
8. Buja LM. Coronary Artery Disease: Pathological Anatomy and Pathogenesis. In: Willerson JT, Holmes DR, editors. Coronary Artery Disease. s.l.: Springer-Verlag; 2015. p. 1–2. doi:10.1007/978-1-4471-2828-1_1.
9. Fumiyuki Otsuka, Masataka Nakano, Frank D. Kolodgie, and Renu Virmani. Evaluation of Vulnerable Atherosclerotic Plaques. In: Willerson JT, Holmes DR, editors. Coronary Artery Disease. s.l.: Springer-Verlag; 2015. p. 409–419.
10. Stefan Agewall. Acute and stable coronary heart disease: different risk factors. European Heart Journal 2008:1927–9.
11. Antoine Lafont. Basic aspects of plaque vulnerability. Heart 2003:1262–7.
12. Aloke V. Finn, Masataka Nakano, Jagat Narula, Frank D. Kolodgie, Renu Virmani. Concept of Vulnerable/Unstable Plaque. Arteriosclerosis, Thrombosis, and Vascular Biology 2010:1282–92.
13. Wikipedia. Angina pectoris - Wikipedia, the free encyclopedia. 10.10.2015. https://en.wikipedia.org/w/index.php?oldid=685097331. Accessed 13 Oct 2015.
14. Robert J. Bache. Coronary Artery Disease: Regulation of Coronary Blood Flow. In: Willerson JT, Holmes DR, editors. Coronary Artery Disease. s.l.: Springer-Verlag; 2015. p. 57–67.
15. Classification of unstable angina and non-ST elevation myocardial infarction. http://www.uptodate.com/contents/classification-of-unstable-angina-and-non-st-elevation-myocardial-infarction. Accessed 22 Oct 2015.
16. James T. Willerson and Paul W. Armstrong. Coronary Heart Disease Syndromes: Pathophysiology and Clinical Recognition. In: Willerson JT, Holmes DR, editors. Coronary Artery Disease. s.l.: Springer-Verlag; 2015. p. 365–407.
17. Payam Safavi-Naeini, Abdi Rasekh, Mehdi Razavi, Mohammad Saeed, and Ali Massumi. Sudden Cardiac Death in Coronary Artery Disease. In: Willerson JT, Holmes DR, editors. Coronary Artery Disease. s.l.: Springer-Verlag; 2015. p. 621–656.
18. Vlodaver Z, Wilson RF, Garry DJ. Coronary Heart Disease: Clinical, Pathological, Imaging, and Molecular Profiles. 1st ed. s.l.: Springer-Verlag; 2012.
19. Windecker S, Kolh P, Alfonso F, Collet J, Cremer J, Falk V, et al. 2014 ESC/EACTS Guidelines on myocardial revascularization: The Task Force on Myocardial Revascularization of the European Society of Cardiology (ESC) and the European Association for Cardio-Thoracic Surgery

(EACTS)Developed with the special contribution of the European Association of Percutaneous Cardiovascular Interventions (EAPCI). European Heart Journal 2014;35:2541–619. doi:10.1093/eurheartj/ehu278.
20. Camm AJ, Lüscher TF, Serruys PW, editors. The ESC textbook of cardiovascular medicine. Malden, Mass.: Blackwell Pub; 2006.
21. Windecker S. CORONARY DISEASE: Intervention in coronary artery disease. Heart 2000;83:481–90. doi:10.1136/heart.83.4.481.
22. Waksman R, Bonello L. The 5 Ts of Bifurcation Intervention: Type, Technique, Two Stents, T-Stenting, Trials Editorials published in JACC: Cardiovascular Interventions reflect the views of the authors and do not necessarily represent the views of JACC: Cardiovascular Interventions or the American College of Cardiology. JACC: Cardiovascular Interventions 2008;1:366–8. doi:10.1016/j.jcin.2008.06.006.
23. Felipe Fuchs VD. Coronary artery bifurcation lesions: A review of contemporary techniques in percutaneous coronary intervention. EMJ Interventional Cardiology 2014;1:73–80.
24. Sukhija R, Mehta JL, Sachdeva R. Present Status of Coronary Bifurcation Stenting. Clin Cardiol 2008;31:63–6. doi:10.1002/clc.20177.
25. Louvard Y, Thomas M, Dzavik V, Hildick-Smith D, Galassi AR, Pan M, et al. Classification of coronary artery bifurcation lesions and treatments: Time for a consensus! Cathet. Cardiovasc. Intervent. 2008;71:175–83. doi:10.1002/ccd.21314.
26. Riccardo Colantonio, Enrico Romagnoli, Giuseppe Sangiorgi. CORONARY BIFURCATION DISEASE AND BIFURCATION STENTING: A PRACTICAL APPROACH. EMJ Interventional Cardiology 2014;1:62–72.
27. Tamburino C. Left Main Coronary Artery Disease: A Practical Guide for the Interventional Cardiologist. Milano: Springer Milan; 2009.
28. Sgueglia GA, Chevalier B. Kissing Balloon Inflation in Percutaneous Coronary Interventions. JACC: Cardiovascular Interventions 2012;5:803–11. doi:10.1016/j.jcin.2012.06.005.
29. Ioannis Iakovou AC. Two-Stent Techniques for the Treatment of Coronary Bifurcations with Drug-Eluting Stents. Hell J of Cardiol 2005;46:188–98.
30. Rainer Wessely GA. Self-Expanding Coronary Stents: Rationale, Clinical Status, Future Prospects. EMJ Cardiol. 2015;3:94–106.
31. Bozsak F, Gonzalez-Rodriguez D, Sternberger Z, Belitz P, Bewley T, Chomaz J, et al. Optimization of Drug Delivery by Drug-Eluting Stents. PLoS ONE 2015;10:e0130182. doi:10.1371/journal.pone.0130182.
32. G. Toth G, Pyxaras S, Mortier P, Vroey F de, Di Gioia G, Adjedj J, et al. Single String Technique for Coronary Bifurcation Stenting. JACC: Cardiovascular Interventions 2015;8:949–59. doi:10.1016/j.jcin.2015.01.037.
33. Regar E, Leeuwen, K. A. H. van, Serruys PW, editors. Optical coherence tomography in cardiovascular research. Abingdon: Informa Healthcare; 2007.
34. Tearney GJ, Regar E, Akasaka T, Adriaenssens T, Barlis P, Bezerra HG, et al. Consensus Standards for Acquisition, Measurement, and Reporting of Intravascular Optical Coherence Tomography Studies. Journal of the American College of Cardiology 2012;59:1058–72. doi:10.1016/j.jacc.2011.09.079.
35. Zhao Wang. Intravascular optical coherence tomography image analysis [Dissertation]: CASE WESTERN RESERVE UNIVERSITY; 2013.
36. Prati F, Guagliumi G, Mintz GS, Costa M, Regar E, Akasaka T, et al. Expert review document part 2: methodology, terminology and clinical applications of optical coherence tomography for the assessment of interventional procedures. European Heart Journal 2012;33:2513–20. doi:10.1093/eurheartj/ehs095.

37. Tyczynski P, Ferrante G, Moreno-Ambroj C, Kukreja N, Barlis P, Pieri E, et al. Simple Versus Complex Approaches to Treating Coronary Bifurcation Lesions: Direct Assessment of Stent Strut Apposition by Optical Coherence Tomography. Revista Española de Cardiología (English Edition) 2010;63:904–14. doi:10.1016/S1885-5857(10)70184-5.
38. Foin N, Torii R, Alegria E, Sen S, Petraco R, Nijjer S, et al. Location of side branch access critically affects results in bifurcation stenting: Insights from bench modeling and computational flow simulation. Int J Cardiol 2013;168:3623–8. doi:10.1016/j.ijcard.2013.05.036.
39. Wikipedia. Coronary artery disease - Wikipedia, the free encyclopedia. 29.09.2015. https://en.wikipedia.org/w/index.php?oldid=683294147. Accessed 30 Sep 2015. [39]

5.2 List of figures

Figure 11: Tearney GJ, Regar E, Akasaka T, Adriaenssens T, Barlis P, Bezerra HG, et al. Consensus Standards for Acquisition, Measurement, and Reporting of Intravascular Optical Coherence

Figure 12: own illustration

Figure 13: adapted from Regar E, Leeuwen, K. A. H. van, Serruys PW, editors. Optical coherence tomography in cardiovascular research. Abingdon: Informa Healthcare; 2007.

Figure 14: own illustration

Figure 15: own illustration

Figure 16: G. Toth G, Pyxaras S, Mortier P, Vroey F de, Di Gioia G, Adjedj J, et al. Single String Technique for Coronary Bifurcation Stenting. JACC: Cardiovascular Interventions 2015;8:949–59. doi:10.1016/j.jcin.2015.01.037.

Figure 17: own illustration

Figure 18: own illustration, screen shot Terumo Lunawave

Figure 19: own illustration, screen shot Terumo Lunawave

Figure 20: own illustration, screen shot Terumo Lunawave

Figure 21: own illustration

Figure 22: own illustration

Figure 23: own illustration

Figure 24: G. Toth G, Pyxaras S, Mortier P, Vroey F de, Di Gioia G, Adjedj J, et al. Single String Technique for Coronary Bifurcation Stenting. JACC: Cardiovascular Interventions 2015;8:949–59. doi:10.1016/j.jcin.2015.01.037.

Figure 25: own illustration

Figure 26: Tyczynski P, Ferrante G, Moreno-Ambroj C, Kukreja N, Barlis P, Pieri E, et al. Simple Versus Complex Approaches to Treating Coronary Bifurcation Lesions: Direct Assessment of Stent Strut Apposition by Optical Coherence Tomography. Revista Española de Cardiología (English Edition) 2010;63:904–14. doi:10.1016/S1885-5857(10)70184-5.

Figure 27: own illustration

5.3 List of abbreviations

AGEP	advanced glycation end products
BMS	bare metal stent
BMI	body mass index
CAD	coronary artery disease
DES	drug eluting stent
DMV	distal main vessel
FD-OCT	Fournier domain optical coherence tomography
FKBI	final kissing balloon inflation
GW	guidewire
HDL	high density lipoprotein
IVOCT	intravascular optical coherence tomography
LAD	left anterior descending
LCX	left circumflex artery
LDL	low density lipoprotein
LMCA	left main coronary artery
MB	main branch
MMP	matrix metalloproteinase
NSTEMI	non-ST-segment elevation myocardial infarction
OCT	optical coherence tomography
OFDI	optical frequency domain imaging
PCI	percutaneous coronary intervention
PMV	proximal main vessel
PTCI	percutaneous transluminal coronary intervention
ROS	reactive oxygen species
SB	side branch
SCD	sudden cardiac death
TCFA	thin-cap fibroatheroma
TD-OCT	time domain optical coherence tomography
UA	unstable angina
VLDL	very low density lipoprotein
VSMC	vascular smooth muscle cell